Accepted Manuscript

2-(phenylthio)ethylidene derivatives as anti-*Trypanosoma cruzi* compounds: Structural design, synthesis and antiparasitic activity

Marcos Veríssimo de Oliveira Cardoso, Gevanio Bezerra de Oliveira Filho, Lucianna Rabelo Pessoa de Siqueira, José Wanderlan Pontes Espíndola, Elany Barbosa da Silva, Andresa Pereira de Oliveira Mendes, Valéria Pereira Hernandes, Maria Carolina Accioly Brelaz de Castro, Rafaela Salgado Ferreira, Filipe Silva Villela, Francielly Morais Rodrigues da Costa, Cassio Santana Meira, Diogo Rodrigo Magalhães Moreira, Milena Botelho Pereira Soares, Ana Cristina Lima Leite

PII: S0223-5234(19)30639-7

DOI: https://doi.org/10.1016/j.ejmech.2019.07.018

Reference: EJMECH 11515

To appear in: *European Journal of Medicinal Chemistry*

Received Date: 29 May 2019

Accepted Date: 6 July 2019

Please cite this article as: Marcos.Verí.de. Oliveira Cardoso, G.B.d. Oliveira Filho, L.R.P.d. Siqueira, José.Wanderlan.Pontes. Espíndola, E.B.d. Silva, A.P.d. Oliveira Mendes, Valé.Pereira. Hernandes, M.C.A.B.d. Castro, R.S. Ferreira, F.S. Villela, F.M.R.d. Costa, C.S. Meira, Diogo.Rodrigo.Magalhã. Moreira, M.B.P. Soares, A.C.L. Leite, 2-(phenylthio)ethylidene derivatives as anti-*Trypanosoma cruzi* compounds: Structural design, synthesis and antiparasitic activity, *European Journal of Medicinal Chemistry* (2019), doi: https://doi.org/10.1016/j.ejmech.2019.07.018.

2-(phenylthio)ethylidene derivatives as anti-*Trypanosoma cruzi* compounds: Structural design, synthesis and antiparasitic activity

Marcos Veríssimo de Oliveira Cardoso[1,*], Gevanio Bezerra de Oliveira Filho[2], Lucianna Rabelo Pessoa de Siqueira[2], José Wanderlan Pontes Espíndola[2], Elany Barbosa da Silva[2], Andresa Pereira de Oliveira Mendes[3], Valéria Pereira Hernandes[3], Maria Carolina Accioly Brelaz de Castro[3,4], Rafaela Salgado Ferreira[5], Filipe Silva Villela[5], Francielly Morais Rodrigues da Costa[5], Cassio Santana Meira[6,7], Diogo Rodrigo Magalhães Moreira[6], Milena Botelho Pereira Soares[6,7] and Ana Cristina Lima Leite[2]

[1] Universidade de Pernambuco, Laboratório de Prospecção de Moléculas Bioativas, Programa de Pós-Graduação em Ciência e Tecnologia Aplicadas no Semiárido, 56328-903, Petrolina, PE, Brazil
[2] Universidade Federal de Pernambuco, Laboratório de Planejamento e Síntese de Fármacos, Departamento de Ciências Farmacêuticas, 50740-520, Recife, PE, Brazil
[3] Fundação Oswaldo Cruz, Centro de Pesquisas Aggeu Magalhães, CEP, 50670-420, Recife, PE, Brazil
[4] Universidade Federal de Pernambuco, Laboratório de Parasitologia, Centro Acadêmico de Vitória - CEP 55608-680, Vitória de Santo Antão, PE, Brazil
[5] Universidade Federal de Minas Gerais, Departamento de Bioquímica e Imunologia, CEP 31270-901, Belo Horizonte, MG, Brazil
[6] Fundação Oswaldo Cruz, Centro de Pesquisas Gonçalo Moniz, CEP 40296-750, Salvador, BA, Brazil
[7] Hospital São Rafael, Centro de Biotecnologia e Terapia Celular, CEP 41253-190, Salvador, BA, Brazil

*To whom correspondence should be addressed: phone +55 (87)3866-6491; e-mail: marcos.cardoso@upe.br

Abstract

Chagas disease is an illness caused by the protozoan parasite *Trypanosoma cruzi*. The current chemotherapy is based on benznidazole, and, in some countries, Nifurtimox, which is effective in the acute phase of the disease, but its efficacy in the chronic phase remains controversial. It can also cause serious side effects that lead sufferers to abandon treatment. In the present work, is reported the synthesis and trypanocidal activity of new 2-(phenylthio)ethylidene thiosemicarbazones (**4**-**15**) and 1,3-thiazoles (**16**-**26**). The cyclization of thiosemicarbazones into 1,3-thiazoles presents an improvement in the cytotoxic profile for *T. cruzi* parasite, denoting selective compounds. Compound **18** was identified as the most promising of all compounds tested, showing an IC_{50} of 2.6 µM for the trypomastigote form and a non-cytotoxic effect on mouse spleen cells, reaching a selective index of 95.1. Among the 22 compounds tested, six compounds present a better trypanocidal activity, and five compounds have an equipotent activity compared to benznidazole. Flow cytometry and ultrastructural analysis were performed and indicate that compound **18** causes parasite cell death through apoptosis and acts via an autophagic pathway.

Keywords: Chagas disease; *Trypanosoma cruzi*; cruzain; thiazoles.

1. Introduction

Chagas disease, a life-threatening illness caused by the protozoan parasite *Trypanosoma cruzi* (*T. cruzi*) has afflicted humanity since its earliest presence in the New World[1] and remains the most significant parasitic disease burden of the American continent[2–4]. *T. cruzi* is a significant public health problem in tropical and subtropical countries, and new chemotherapies are highly needed. It is estimated that approximately 6-7 million people worldwide are infected with *T. cruzi*, mainly in Latin America[5].

Current specific chemotherapy is based only on two compounds, nifurtimox (**Nfx**) and benznidazole (**Bdz**), which were developed empirically over 40 years ago[6] and are associated with long-term treatments, severe side effects and low access worldwide [7,8]. **Nfx** and **Bdz** can eliminate patent parasitemia and reduce serological titers in acute and early chronic infections[9,10], but they have low efficacy in prolonged chronic infections[11,12].

Among the drug targets being investigated for Chagas disease, cruzain[13–16] is its most abundant cysteine protease and is essential for parasite survival[17]. Cruzain is a cathepsin-L-like protease of the papain family, relevant for intracellular replication and differentiation of *T. cruzi* parasites[18]. Activity levels are highest in epimastigotes and, depending on the life cycle stage, cruzain can be found on the cell surface of *T. cruzi* amastigotes or lysosome-like organelles present on *T. cruzi* epimastigotes called reservosomes[19]. In addition to its role in parasite nutrition, cruzain has been implicated in many cellular processes, including cell invasion, proliferation, parasite differentiation, metacyclogenesis and evasion of the host immune response[18].

1,3-Thiazole is one of the most remarkable scaffolds in heterocyclic chemistry, drug design and discovery. It is found in a plethora of pharmacologically active substances and naturally occurring compounds. Thiazole is a versatile building block for lead generation, easily yielding access to diverse derivatives for subsequent lead optimization. In recent years, thiazole derivatives have been synthesized and shown to possess varied biological activities[20]. 1,3-thiazoles and their analogues have been examined as antiparasitic agents, especially against Chagas disease[21–23]. As seen in compounds previously synthesized by our group (**Scheme 1**), the first generation of thiazolin-4-ones was planned with a 2-(phenylthio)ethylidene linked at N1. Further compounds explored a halogen exchange and the modification of sulfur to oxygen. The next structural improvement was the scaffold hopping from thiosemicarbazone (**9**) to the thiazolin-4-one moiety (**6f**), providing better trypanocidal activity (IC_{50}: 101.9 vs 0.3 µM)[24]. The importance of the bioisosteric replacement of thiazolin-4-one (**18**) by a 1,3-thiazole (**29**) was also investigated, leading to less cytotoxic and more active compounds against parasites (trypomastigote and epimastigote forms)[25]. The use of the spacer group "-CH_2-CH_2-CH=" between the 2-(phenylthio)ethylidene and N1 was also explored, however, no improvement in trypanocidal activity was observed[26].

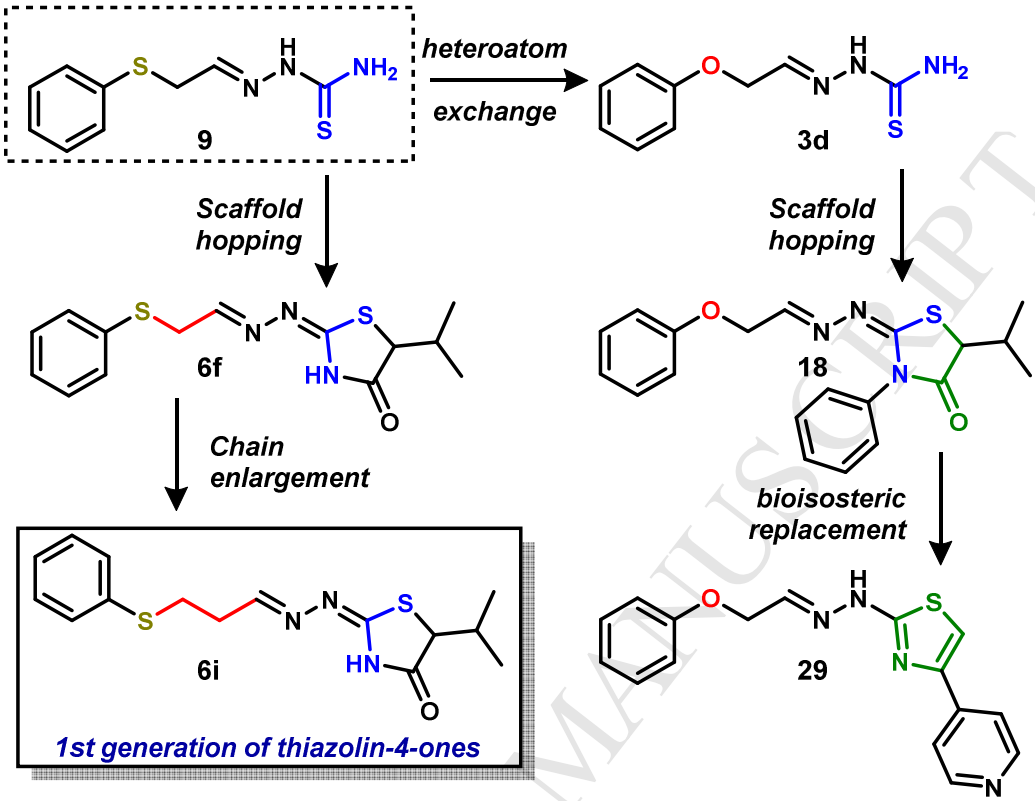

Scheme 1. Structural planning of previously compounds synthesized by our group.

The good results achieved by thiazolin-4-one and 1,3-thiazole derivatives as anti-*T. cruzi* agents motivate us to investigate the trypanocidal activity of new 1,3-thiazoles possessing different 2-(phenylthio)ethylidene groups attached at N1 (**Scheme 01**)[23–30].

The search for less toxic and more potent compounds is a constant goal of the medicinal chemistry. In this work, it was explored the trypanocidal activity of new 1,3-thiazoles, applying substitutions with different 2-(phenylthio)ethylidenes at N1 and the scaffold hopping of thiosemicarbazone to 1,3-thiazole, substituted with aromatic rings attached at C4 (**Fig 01**).

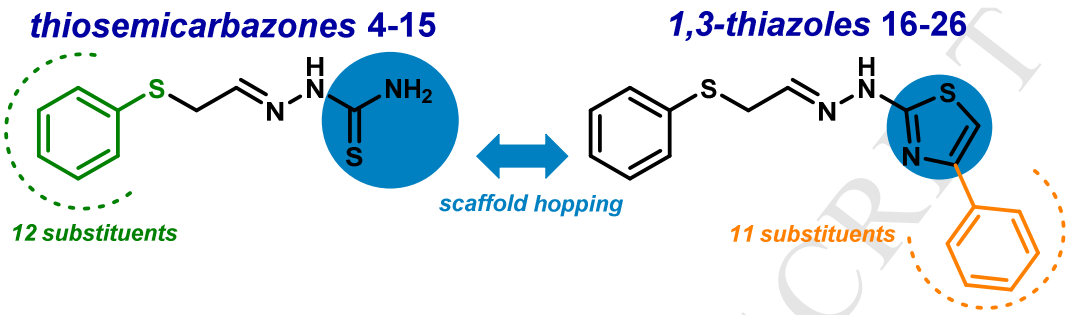

Figure 1. Main structural modifications proposed in this work.

In this work, is report the synthesis, trypanocidal activity, and primary structure-activity relationships (SAR) of a series of 2-(phenylthio)ethylidene thiosemicarbazones (**4-15**) and functionalized 1,3-thiazoles (**16-26**). Compounds (**4-26**) were assayed for their *in vitro* anti-*T. cruzi* activity against the epimastigote and trypomastigote forms. The most active compounds were also evaluated against the intracellular form of the parasite. Their cytotoxicity in mammalian cell cultures was also investigated. The investigation of cruzain as a possible target for (**4-26**) was also performed. To a better understanding of the mechanism of action of the proposed compounds, cell viability, and confocal microscopy studies were also undertaken.

2. Results and Discussion

2.1.Chemistry

Thiosemicarbazones (**4-15**) were prepared by reacting commercially available thiosemicarbazide with the respective 2-(phenylthio)acetaldehyde (**3**) (1:1.2 mol ratio) under ultrasound irradiation in the presence of a catalytic amount of acetic acid. This

protocol led to yields in the range of 30-40%. 1,3-thiazoles (**16-26**) were prepared via Hantsch cyclization between thiosemicarbazone (**4**) and substituted α-bromoacetophenones (**Scheme 2**). These reactions proceed upon refluxing with ethanol (2-4 h), but we adapted them under ultrasound conditions[31] using 2-propanol as solvent[32] and observed yield ranges of 50-85% and shorter reaction times (60 min in most cases), compared with the reflux protocol.

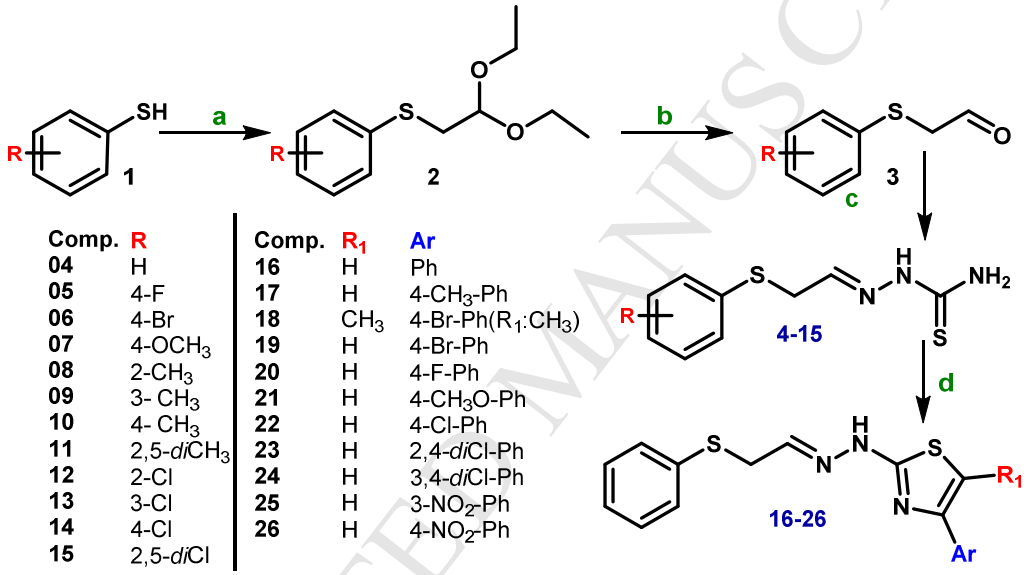

Comp.	R
04	H
05	4-F
06	4-Br
07	4-OCH_3
08	2-CH_3
09	3- CH_3
10	4- CH_3
11	2,5-*di*CH_3
12	2-Cl
13	3-Cl
14	4-Cl
15	2,5-*di*Cl

Comp.	R_1	Ar
16	H	Ph
17	H	4-CH_3-Ph
18	CH_3	4-Br-Ph(R_1:CH_3)
19	H	4-Br-Ph
20	H	4-F-Ph
21	H	4-CH_3O-Ph
22	H	4-Cl-Ph
23	H	2,4-*di*Cl-Ph
24	H	3,4-*di*Cl-Ph
25	H	3-NO_2-Ph
26	H	4-NO_2-Ph

Scheme 2. Synthetic procedures for compounds **4-15** and **16-26**.

Reagents and conditions: (a) K_2CO_3, bromoacetaldehyde diethyl acetal, ultrasound, 40°C, 120 min; (b) H_2SO_4 10%, ultrasound, r.t., 120 min. (c) thiosemicarbazide, ethanol, acetic acid (3 drops), ultrasound, 40°C, 120 min; (d) respective α-bromoacetophenone (2,4´-dibromopropiophenone for compd. **18**), calcium carbonate, 2-propanol, ultrasound, r.t., 60 min.

2.2. Cytotoxicity

After chemical characterization, the cytotoxic profile against BALB/c mouse splenocytes (**Table 1**) was measured as the per cent of ^{3}H-thymidine incorporation for treated cells in comparison to untreated cells. The highest non-cytotoxic concentration was determined by the average of triplicates (**Table 1**).

Table 1. Anti *T. cruzi* activities of thiosemicarbazones **04-15** and 1,3-thiazoles **16-26**.

Compd.	Ar	*T. cruzi*, IC_{50} (μM) trypomastigote[a]	epimastigote[b]	Toxicity splenocytes[c]	SI[d]
		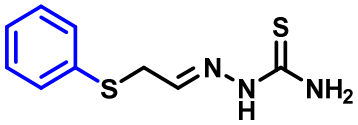			
04	Ph	89.0	101.9	22.2	0.25
05	4-FPh	5.7	6.1	20.5	3.6
06	4-BrPh	6.6	15.4	<3.3	0.5
07	4-CH_3OPh	39.7	32.1	<3.9	0.1
08	2-CH_3Ph	6.1	15.3	41.8	6.9
09	3-CH_3Ph	1.8	6.3	<4.2	2.3
10	4-CH_3Ph	ND	9.6	4.2	ND
11	2,5-*di*CH_3Ph	5.9	6.2	<3.9	0.7
12	2-ClPh	6.2	47.7	<3.8	0.6
13	3-ClPh	14.1	5.5	96.2	6.8
14	4-ClPh	14.1	6.2	<3.8	0.3
15	2,5-*di*ClPh	8.2	6.1	85.0	10.4
		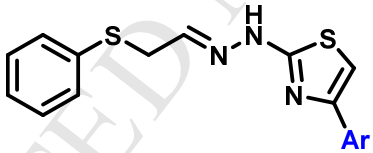			
16	Ph	5.2	59.4	153.6	29.5
17	4-CH_3Ph	5.7	9.4	147.3	25.8
18	4-BrPh	2.6	4.1	>247.3	95.1
19	4-BrPh	14.3	5.4	>239.0	16.7
20	4-FPh	41.7	ND	>291.2	7.0
21	4-CH_3OPh	18.5	62.7	>281.3	15.2
22	4-ClPh	4.1	6.8	>277.8	67.8
23	2,4-*di*ClPh	4.1	7.9	126.8	30.9
24	3,4-*di*ClPh	15.2	56.5	126.8	8.3
25	3-NO_2Ph	19.2	8.4	135.0	7.0
26	4-NO_2Ph	8.4	16.0	67.5	8.0
Bdz	---	6.2	6.6	96.1	15.5

[a] Determined 24 h after incubation of trypomastigotes with the compounds. [b] Determined five days after incubation of epimastigotes with the compounds. IC_{50} was calculated from at least five concentrations, in duplicate (SD ± 10%). [c] Highest nontoxic concentration for mouse splenocytes after 24 h of incubation in the presence of the compounds. [d] Selectivity index = toxicity splenocytes / IC_{50} trypomastigotes. **Bdz**: benznidazole. ND: not determined.

Overall, tested thiosemicarbazones showed toxicity higher than **Bdz**, except for **13** and **15**, that present similar toxicity. Otherwise, 1,3-thiazoles present a significant improvement in the toxicity profile by comparison to thiosemicarbazones **4-15**, probably due to the cyclization of thiocarbonyl to a 1,3 thiazole group (**Table 1**), these findings are in agreement with previous results[23,24,26,33–35]. The most of 1,3-thiazole derivatives tested present lower toxicity than **Bdz**, except for compound **26** (4-nitro derivative) (**Table 1**).

2.3. Antiparasitic activity against extracellular forms

Derivatives **4-15** and **16–26** were evaluated *in vitro* against the epimastigote and trypomastigote forms of *T. cruzi* in a screening scheme that included five different concentrations (1.2, 3.7, 11.1, 33.3, and 100 μg/mL). Their ability to inhibit parasite growth was tested in comparison to the standard drug (**Bdz**). The selective index was measured only for compounds that present cytotoxicity higher than 100 μM.

In view to state the influence of the arylthio group in the trypanocidal activity, a comparison between previously synthesized compounds bearing arylthio and alkoxy group was made, as expressed in **Fig. 2** that present potent arylthio and alkoxy derivatives. HERNANDES *et al*. demonstrated the synthesis and anti. *T. cruzi* profile of 23 compounds, being twelve thiosemicarbazones and eleven 1,3-thiazoles, and identified potent compounds for anti-*T. cruzi* activity, however, none of them was more potent than lead compound (**18**). Another important work in this field is described by MOREIRA *et al*., which presented 38 compounds, exploring thiazolin-4-one and 1,3-thiazole ring. Those molecules possess an alkoxy group instead arylthio group, performing high activity against epimastigotes and trypomastigotes of *T. cruzi*; however, the most active compounds did not

overlap compound **18**, denoting the importance of the arylthio group. The compound **34** presented by Moreira et al. have significant structural similarity to compound **18**, differing only by a methyl at **C3** and an alkoxy instead of an arylthio group; This demonstrates the benefits of the arylthio group over alkoxy group, due to a 10-fold more potency against epimastigote form.

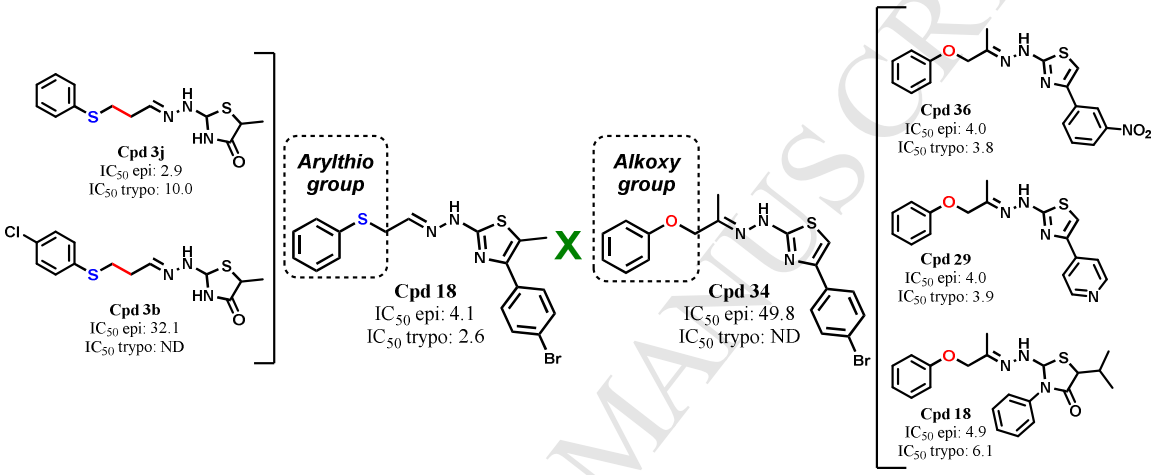

Figure 2. Comparison of *T. cruzi* activity of arylthio and alkoxy groups.

To discuss the importance of the cyclization of thiocarbonyl into 1,3-thiazole is first compared to the results of anti-*T. cruzi* activity against the trypomastigote form of the non-substituted thiosemicarbazone **4** (89.0 μM) with the non-substituted 1,3-thiazole **16** (5.2 μM). It can be observed that compound **16** is 17-fold more potent than **4**, demonstrating the importance of the cyclization. Indeed, compound **4** is 14-fold less potent than **Bdz**, followed by thiosemicarbazones **7**, **13**, and **14**. However, compounds **5** (5.7 μM), **6** (6.6 μM), **8** (6.1 μM), **11** (5.9 μM), **12** (6.1 μM) and **15** (8.2 μM) present equipotent trypanocidal profile to **Bdz** (6.2 μM) (**Table 1**). Analyzing *para*-substituted compounds **5-7**, **10** and **14**, is noted that the insertion of substituents at C4 provides a significant

improvement in trypanocidal activity, in comparison to the non-substituted compound **4**. The insertion of fluorine at C4 (**5**) leads to the most active compound, giving a significant improvement in anti-*T. cruzi* activity (trypomastigote form), being 15-fold more potent than compound **4** (IC_{50} 5.7 vs 89.0 μM). About methyl-substituted compounds **8**-**11**, it was noticed that **8** is equipotent to dimethyl-substituted **11**, but it has 10-fold less toxicity. Compound **9** is the most active methyl substituted compound and, compared with compound **4**, it exhibits an incredible 49-fold improvement of the IC_{50}, being the most active thiosemicarbazone evaluated in this work. However, it also presents toxicity to BALB/c splenocytes, leading to a low selective index. For chlorine-substituted **12**-**15**, it was observed a good improvement in the trypanocidal activity, with **13** being the most active for the epimastigote form. Comparing compounds **11** and **15**, both disubstituted at 2,5 positions with methyl (**11**) and chlorine (**15**), respectively, is observed an equipotency in the trypanocidal activity, but derivative **15** shows lower cytotoxicity.

Among the twelve thiosemicarbazones derivatives assayed, seven are equipotent to benznidazole, with compound **9** being the most active, exhibiting an IC_{50} of 1.8 μM against the trypomastigote form (**Table 1**). However, compound **15** presents similar toxicity and trypanocidal activity to benznidazole, making it the most promising thiosemicarbazone evaluated in this study. About the 1,3-thiazole derivatives, trypanocidal activities (trypomastigote) of *para*-substituted compounds were first compared with that of compound **16** (non-substituted).

Compound **16** shows a trypanocidal activity equivalent to **Bdz**, with lower cytotoxicity. Comparing *para*-substituted compounds (**17**-**22** and **26**) with **16** was observed an improvement in the cytotoxicity profile, except for compound **17**, which shows similar

trypanocidal and toxicity activities, and **26**, which shows increased toxicity. With respect to the trypanocidal activity, a substantial increment was observed for compounds **18** (2.6 μM) and **22** (4.1 μM), while **17** (5.7 μM), **19** (14.3 μM), **20** (41.7 μM), **21** (18.5 μM) and **26** (8.4 μM) were less effective than **16** (5.2 μM).

Predominantly, the insertion of substituents at the *para* position did not increase the trypanocidal activity, but maintained or decreased the toxicity, especially the chlorine (**22**) and bromine-substituted (**18**) compounds, which showed both low toxicity levels (>100 μM) and potent trypanocidal activity, leading to a high selective index (SI). Nitro compounds, *meta* (**25**) and *para* (**26**) substituted, show lower trypanocidal activities than **16**, with compound **25** presenting a better toxicity level (135 μM against 67.5 μM) and lower trypanocidal activity (19.22 μM against 8.45 μM) than compound **26**. Attachment of a methyl group at C5 in the 1,3-thiazole ring improved the trypanocidal activity, as shown by the comparison between compounds **18** and **19**, both bromine-substituted.

In overall, about the trypanocidal activity of 1,3-thiazoles **16**-**26** (**Table 1**), the most viable compounds were **18** and **22**, presenting higher SI than **Bdz**. Aim In **Fig. 2**, the relationships between compounds **18**, **22**, and **23** and their drug likenesses[36] are measured; however, no clear correlation can be established.

2.4.Antiparasitic activity against the intracellular form

Aiming at a better understanding of the trypanocidal activity of 1,3-thiazoles, was evaluated the effect of the compounds on trypomastigote invasion and development, as these events are crucial for the establishment of the disease in mammalian hosts[37,38]. Chemically inhibiting parasite invasion and growth are desirable functional properties for any Chagas

disease drug candidate. For that reason, it was performed *in vitro* experiments on Y strain trypomastigotes in mouse macrophages[39]. Non-cytotoxic compounds with trypanocidal activities higher than that of **Bdz** were selected for the evaluation of *in vitro* assays of infection by *T. cruzi* (**Fig. 3**).

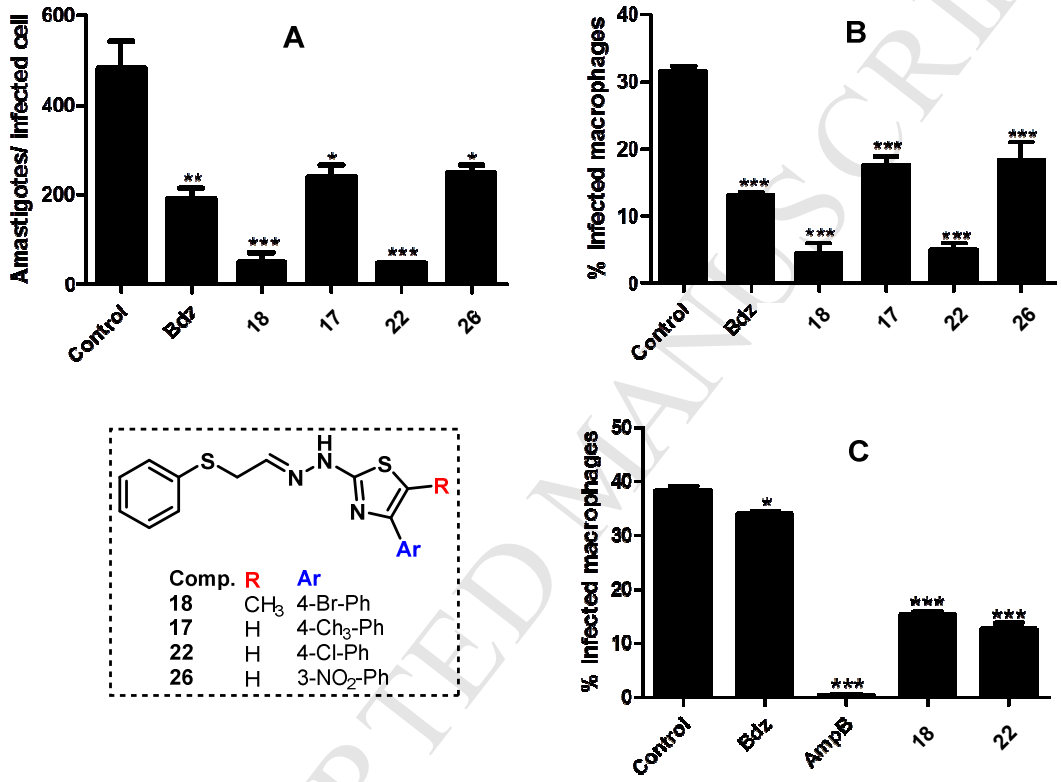

Figure 3. *T. cruzi*-infected macrophages were treated and incubated for three days. A) Mean the number of intracellular amastigotes per 100 infected macrophages. B) Infected cells in per cent. C) Macrophages were simultaneously exposed to trypomastigotes and treatment. The cell culture was incubated for 2 h and washed, and the per cent of infected cells was determined after 2 h. Bdz= benznidazole, AmpB = amphotericin B. Data are the mean ± S.E.M. (error bars) of two independent experiments performed. Panels A and B: ***, P <0.001; panel C: ***, P <0.001; **, P <0.01.

Macrophages previously infected with Y strain trypomastigotes were treated with 20 µM of compounds **17**, **18**, **22** and **26**. Cells were stained with Giemsa and observed by optical microscopy to evaluate the percentage of infected macrophages and the relative number of amastigotes per 100 cells. As shown in **Fig. 3**, the treatment with 1,3-thiazoles significantly decreased the percentage of infected macrophages (P < 0.05) and the relative number of

amastigotes per 100 macrophages ($P < 0.05$) when compared with untreated cultures. When tested at different concentrations, it was possible to calculate the IC_{50} value of 1,3-thiazoles against intracellular amastigotes. Compounds **18** and **22** presented IC_{50} values of 10.15 (±0.98) µM and 7.88 (±0.03) µM, respectively, demonstrating an activity superior to that of **Bdz** in inhibiting infection (**Fig 3A** and **3B**). Compounds **17** and **26** presented a moderate activity, with IC_{50} values of 18.78 (±0.03) µM and 19.26 (±0.53) µM, respectively.

It was also evaluated the effect of 1,3-thiazoles on the invasion process. In this assay, mouse macrophages were exposed to trypomastigotes and at the same time were treated with the 1,3-thiazoles (20 µM) for 2 h. After this time, the cells were washed with saline solution to remove extracellular parasites and incubated for 2 additional hours. Cells were stained with hematoxylin and eosin and analyzed by optical microscopy. Amphotericin B was used as a positive control for this experiment. As shown in **Fig. 3C**, 1,3-thiazoles significantly inhibited the parasite invasion in comparison to untreated cells ($P < 0.001$) but not as efficiently as the positive control amphotericin B. However, they were more effective than benznidazole, which shows a weak activity on this assay.

2.5. Cruzain inhibition activity

The thiosemicarbazones and their cyclic analogues 1,3-thiazoles were tested against the enzyme cruzain the *T. cruzi* in view to investigate the probable mechanism of action. The inhibition of cruzain enzymatic activity by all compounds was measured using a competition-based assay with the fluorescent substrate Z-Phe-Arg-aminomethylcoumarin (Z-FR-AMC)[40]. All compounds were screened at 100 µM, and only compounds having an inhibition value of >70% were chosen to determine their IC_{50} values. Therefore, in some

cases, the discussion was performed in terms of the percentage of cruzain inhibition (**Table 3**).

Table 3. *In vitro* cruzain inhibition activity of compounds **04-26**.

Compound	% Cruzain Inhibition (100 µM)[a]	Compound	% Cruzain Inhibition (100 µM)[a]
04	42.1 ± 5.6	**16**	ND
05	27.5 ± 3.3	**17**	11.9 ± 2.8
06	16.6 ± 3.5	**18**	27.0 ± 2.4
07	34.6 ± 3.4	**19**	7.0 ± 2.2
08	13.9 ± 3.2	**20**	22.9 ± 2.3
09	43.4 ± 5.2	**21**	ND
10	31.4 ± 4.4	**22**	17.6 ± 4.8
11	87.6 ± 2.3 (3.3 ± 2.6[b])	**23**	67.2 ± 5.4
12	46.0 ± 5.4	**24**	62.9 ± 4.5
13	75.9 ± 2.3 (19.0 ± 15.2[b])	**25**	16.2 ± 2.8
14	25.2 ± 6.0	**26**	18.9 ± 3.8
15	37.4 ± 5.8		

[a] Average values and standard errors were calculated based on five independent experiments, performed in triplicate. [b]Average and standard errors were calculated based on two independent curves, each including at least seven compound concentrations in triplicates. IC_{50} (µM) are given in parenthesis. Standard errors were calculated based on the formula $\sigma/\sqrt{n}$, where σ is the standard deviation and n is the number of measurements.

Cruzain inhibition by thiosemicarbazones was first reported by Du et al.[41]. The suggested mechanism of inhibition involves a nucleophilic attack at the thiocarbonyl group by the catalytic Cys25 residue and electron delocalization to the sulfur atom, which is stabilized by the neighbouring His159[41]. Based on the importance of the sulfur highlighted by this work, it was evaluated several thiosemicarbazones with a spacer group containing a sulfur atom to investigate a possible increment in the cruzain inhibition. Substitution of the

unsaturated sulfur in the thiocarbonyl group with saturated cyclic sulfur on the 1,3-thiazole ring, along with the cyclization of thiosemicarbazone to 1,3-thiazole, was also investigated.

Of thiosemicarbazones **4-15**, only two compounds (**11** and **13**) show cruzain inhibition higher than 70% at 100 μM (87.6 and 75.9%, respectively), presenting IC_{50} values of 3.3 ± 2.6 and 19.0 ± 15.2 μM, respectively. In comparison to compound **4**, only compounds **11** and **13** show increments in the cruzain inhibition. The difference between compounds **11** and **13** is that **11** is substituted in positions 2,5 by a methyl group, while **13** is substituted by a chloro group at the *meta* position. In addition to the orientation of the substituents, the main difference is that **13** has an electron-withdrawing substituent, whereas **11** has donor substituents. However, this trend is not observed in other compounds with withdrawing/donor substituents.

Of cyclic compounds **16**-**26**, none of them present inhibition rates greater than 70% at 100 μM, so the IC_{50} values were not measured. In the comparison of 1,3-thiazoles with the lead thiosemicarbazone **4**, it is noted that only compounds **23** and **24** present better inhibition rates (67.2 ± 5.4 and 62.9 ± 4.5 vs 42.1 ± 5.6, respectively). These results indicate that the trypanocidal activity of these compounds is due to another mechanism of action. This result is not in agreement to previous findings that suggest that thiosemicarbazones and 1,3-thiazoles are inhibitors of cruzain[28,30], which as not observed in this work. Furthermore, studies of cell death and ultra-structural analysis were performed, aiming at a better understanding of the mechanism of action.

2.6. Flow cytometry analysis

After confirming that the compounds can kill parasites, the next step was to understand how they affect parasite cells through assays with the trypomastigote form of *T. cruzi* treated with MBHA3. Understanding the mechanism involved may provide insights into the pathogenesis of Chagas disease and help to develop better therapies against this illness.

Evaluation of apoptosis and necrosis by flow cytometry is usually accomplished by the combined use of annexin V (AV) - FITC and PI. Annexin V - FITC accesses phosphatidylserine molecules exposed on the external membrane in the early stage of apoptosis, and PI allows the identification of nuclear alterations in the late stages of apoptosis or necrosis, as a consequence of the increase in membrane permeability[42–44]. Most cells positive for AV were also PI positive, suggesting that apoptotic cells evolved into secondary necrosis. However, we cannot rule out the possibility that annexin might also bind to the inner phosphatidylserine residues after the membrane integrity has been lost. As shown in **Fig. 4**, when compared with untreated cells, most of the parasite cells treated with thiosemicarbazones were positively stained for AV and PI. Therefore, we suggest that 1,3-thiazole-based treatment causes parasite cell death through apoptosis.

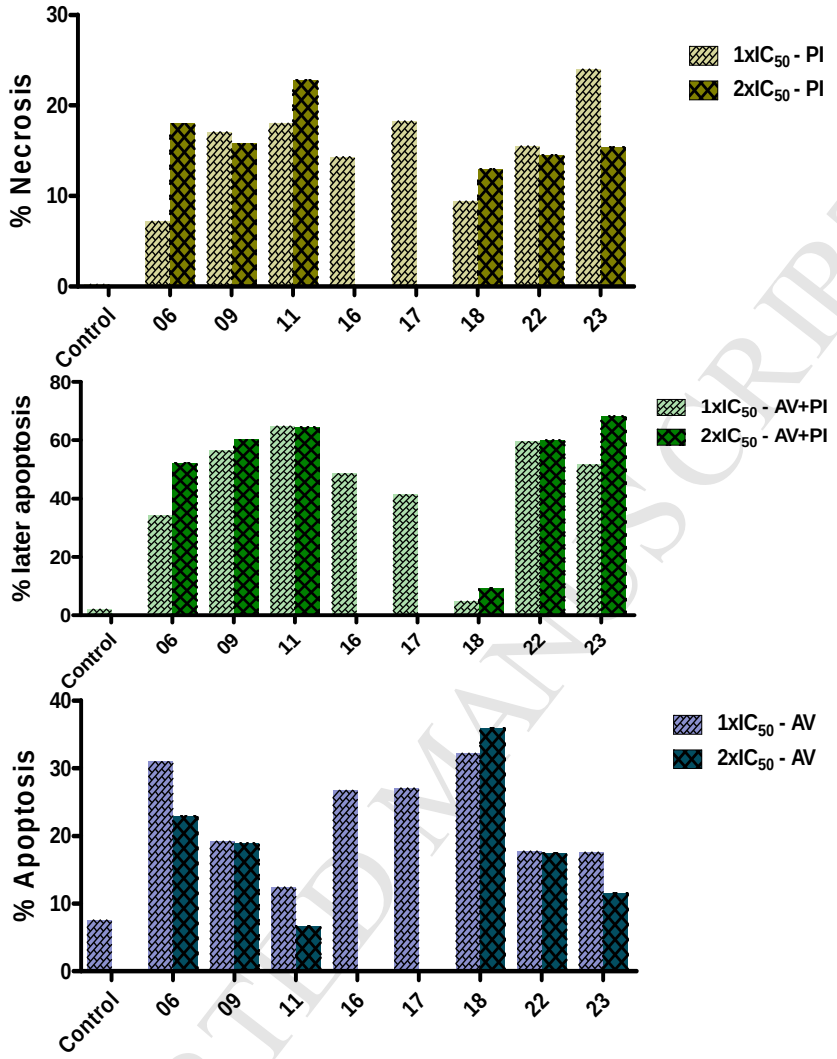

Figure 4. Effects of compound **06**, **09**, **11**, **17**, **18**, **22** and **23** treatments on Annexin V/PI labelling.

2.7. Ultra-structural analysis

To investigate the mechanism of action of compound **18**, ultrastructural alterations in bloodstream trypomastigotes were also analyzed. As shown in **Fig. 5A**, thin sections of untreated trypomastigotes observed by TEM revealed a typical appearance of organelles, intact plasma membrane and parasite cytoplasm without alterations. However, the treatment with compound **18** at 3.0 μM for 24 h caused disorganization of the Golgi complex (**Fig. 5B**), the appearance of numerous atypical vacuoles in the cytoplasm (**Fig. 5C**) and the

appearance of myelin figures within the mitochondria and in the cytoplasm. Vacuole formation and the presence of myelin-like figures are commonly associated with the process of autophagy[45,46]. This might be indicative that the trypanocidal activity of compound **18** can be, in part, assigned to the activation of autophagic pathways.

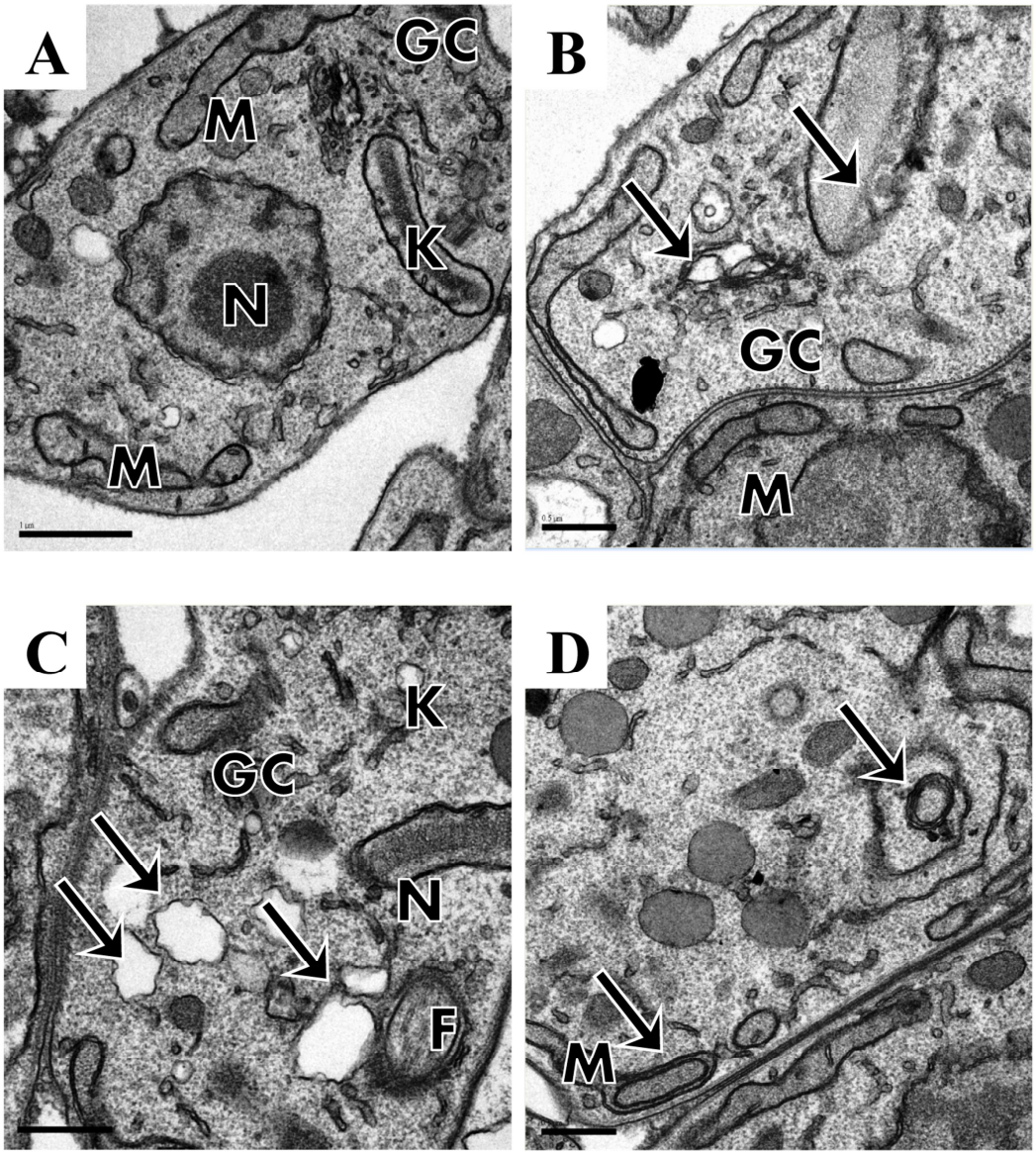

Figure 5. Transmission electron micrographs of trypomastigotes treated or not with compound **18** for 24 hours. (A) Shows an image of untreated trypomastigotes, presenting a typical morphology of the nucleus (N), kinetoplast (K), mitochondria (M) and Golgi complex (GC). Treatment with compound **18** at 3 μM (B-D) induces Golgi complex disorganization (B), appearance of atypical vacuoles in the cytoplasm (C) and the appearance of myelin Figs within the mitochondria and in the

cytoplasm (D). Black arrows indicate alterations from parasites. Scale bars: A = 1 μm; B-D = 0.5 μM.

2.8.Physicochemical properties

For a better analysis of the synthesized compounds, the online software SwissADME (a free web tool to evaluate pharmacokinetics, drug-likeness and medicinal chemistry friendliness of small molecules) was used to determine the physicochemical descriptors and define the pharmacokinetic properties and drug-like nature of all compounds. Physicochemical properties were important to determine if they agree with Lipinski's rule [36,47]. This rule has essential determinants in providing better pharmacokinetics and analyzes promising future drug development. Compound following at least three of the four criteria are considered to adhere to the Lipinski Rule [36]. All synthesized compounds are compatible with Lipinski Rule. Another attractive property is the number of rotatable bonds and the polar surface area (PSA). A large number of rotatable bonds (≥10) has been associated with poor oral bioavailability [48]. Compounds with a low PSA (≤ 140 $Å^2$) tend to have higher oral bioavailability [48,49]. All synthesized compounds have appropriate PSA and number of rotatable bonds (**Table 4**).

Table 4: Physicochemical property profile of derivatives (**4-26**), calculated by SwissADME web tool (http://www.swissadme.ch/index.php)

CPD.	MW (g/mol) <500	MLog P <=4.15	H-bond donors <5	H-bond acceptors <10	Lipinski violations	#Rotatable bonds <10	TPSA <=140
4	225.33	1.69	2	1	0	5	107.8
5	243.32	2.11	2	2	0	5	107.8
6	304.23	2.41	2	1	0	5	107.8
7	255.36	1.41	2	2	0	6	117.0
8	239.36	1.99	2	1	0	5	107.8
9	239.36	1.99	2	1	0	5	107.8
10	239.36	1.99	2	1	0	5	107.8
11	253.39	2.28	2	1	0	5	107.8
12	259.78	2.26	2	1	0	5	107.8
13	259.78	2.26	2	1	0	5	107.8
14	259.78	2.26	2	1	0	5	107.8
15	294.22	2.82	2	1	0	5	107.8
16	325.45	3.37	1	2	0	6	90.8

17	339.48	3.61	1	2	0	6	90.8
18	418.37	4.23	1	2	1	6	90.8
19	404.35	4	1	2	0	6	90.8
20	343.44	3.76	1	3	0	6	90.8
21	355.48	3.03	1	3	0	7	100.0
22	359.90	3.88	1	2	0	6	90.8
23	394.34	4.38	1	2	1	6	90.8
24	394.34	4.38	1	2	1	6	90.8
25	370.45	3.17	1	4	0	7	136.6
26	370.45	3.17	1	4	0	7	136.6
Bdz	260.25	0.37	1	4	0	6	92.7

As demonstrated in **Table 5**, the most active compounds shown variable permeability based on gastrointestinal absorption (GI), according to the BOILED-Egg predictive model (Brain Or IntestinaL EstimateD permeation method). The toxicity result of the drug from SwissADME shows it to be very soluble in the body, it also has a high Gastrointestinal Tract (GI) absorption, and the drug was not blood-brain barrier permanent. These are important as it would allow the drug to have high uptake. The most selective derivatives showed high gastrointestinal absorption (**18**, **22**, and **23**). Concerning oral bioavailability, it has expected 0.55 of the probability of oral bioavailability score > 10% in the rat for all compounds, similar to **Bdz**. All these data suggest a good in silico drug-likeness profile and high chemical stabilities for all compounds synthesized.

Table 5: ADME properties of most active compounds.

Compound	*BBB permeant	**GI absorption	Bioavailability Score
18	No	High	0.55
22	No	High	0.55
23	No	High	0.55
Bdz	No	High	0.55

*BBB - blood-brain barrier.
**GI - Gastrointestinal absorption.

3. Conclusion

In conclusion, the functionalization of thiosemicarbazones (**4-15**) to thiazoles (**16-26**) resulted in a better cytotoxicity profile, as the cyclic analogues showed an improved

selectivity index. Comparing compounds **4** to **16**, unsubstituted representatives of thiosemicarbazone and 1,3-thiazole groups, there was observed an 18-fold improvement in the trypanocidal activity (trypomastigote form), suggesting the importance of the functionalization of thiocarbonyl to a thiazole moiety. Compound **18** is the most promising candidate an anti-*T. cruzi* drug, being non-toxic for splenocytes at the highest dose tested (247.8 µM) and keeping high trypanocidal activity. Besides, ultrastructural studies and flow cytometry analysis revealed ultrastructural alterations induced by the 1,3-thiazoles, which at first result in apoptotic parasite cell death.

4. Experimental section

4.1. General

All reagents were purchased from commercial sources (Sigma-Aldrich, Vetec, or Fluka). Progression of the reactions was followed by thin-layer chromatography (TLC) analysis (Merck, silica gel 60 F_{254} in aluminium foil). The purity of the target compounds was confirmed by combustion analysis (for C, H, N, S) performed by a Carlo-Erba instrument (model EA 1110). Melting points were determined on a Fisatom 430D electrothermal capillary melting point apparatus and were uncorrected. NMR spectra were measured on either a Varian UnityPlus 400 MHz (400 MHz for ^{1}H and 101 MHz for ^{13}C) or a Bruker AMX-300 MHz (300 MHz for ^{1}H and 75.5 MHz for ^{13}C) instrument. DMSO-d_6 and D_2O were purchased from CIL or Sigma-Aldrich. Chemical shifts (δ) are reported in ppm. Multiplicities are given as s (singlet), d (doublet), t (triplet), m (multiplet), dd (double doublet), and coupling constants (*J*) in Hertz. Mass spectrometry experiments were performed on an LC-IT-TOF (Shimadzu). Unless otherwise specified, ESI was carried out in positive ion mode. Typical conditions were a capillary voltage of 3 kV, a cone voltage of

30 V, and a peak scan between 50-1000 *m*/z. IR spectra were recorded with a Bruker model IFS66 FT-IR spectrophotometer using KBr pellets.

4.2.General procedure for the synthesis of thiosemicarbazones (**4-15**)

Example for compound (**4)**: to a solution aldehyde (**3**) (0.76 g, 5 mmol) in ethanol (10 mL) was added thiosemicarbazide (0.46 g, 5 mmol) and a few drops of acetic acid. The reaction vessel was placed in an ultrasonic bath (40 MHz, 180 V) and irradiated for 120 min at r.t. The precipitate was filtered, washed with hexane, and then dried in a desiccator under vacuum. An additional amount of the desired compound could be recovered from the filtrate after cooling.

4.2.1. 2-[(2-phenylthio)ethylidene] thiosemicarbazone (**4**)

Crystallization from toluene/hexane 7:3, afforded white crystals, yield = 86%. Mp (ºC): 125-126. IR (KBr): 1595 (C=N), 3247 (NH), 3390 (NH_2) cm^{-1}. ^1H NMR (300 MHz, DMSO-d_6) δ 3.78 (d, *J* = 6.0 Hz, 2H, S-CH_2), 7.19 (t, *J* = 7.2 Hz, 1H, N=CH), 7.31 (t, *J* = 6.6 Hz, 2H, Ar), 7.34 (t, *J* = 6.1 Hz, 1H, Ar), 7.38 (d, *J* = 7.2 Hz, 2H, Ar), 7.54 (s, 1H, NH_2), 8.09 (s, 1H, NH_2), 11.19 (s, 1H, NH). ^{13}C NMR (75 MHz, DMSO-d_6) δ 33.5 (S-CH_2), 126.1 (C-Ar), 128.4 (C-Ar), 129.0 (C-Ar), 134.6 (C-Ar), 141.5 (C=N), 177.8 (C=S). HRMS (ESI): 226.0491 $[M + H]^+$. Anal. Calcd for $C_9H_{11}N_3S_2$: C, 47.97; H, 4.92; N, 18.65; S, 28.46; found: C, 47.80; H, 5.09; N, 18.61; S, 28.50.

4.2.2. 2-{2-[(4-fluorophenyl)thio]ethylidene} thiosemicarbazone (**5**)

Crystallization from toluene/hexane 7:3, afforded yellow crystals, yield = 39%. Mp (ºC): 106-108. IR (KBr): 1591 (C=N), 3258 (NH), 3404 (NH_2) cm^{-1}. ^1H NMR (300 MHz,

DMSO-d_6) δ 3.74 (d, J = 6.0 Hz, 2H, S-CH_2), 7.32 (t, J = 6.0 Hz, 1H, N=CH), 7.42 (d, J = 5.3 Hz, 2H, Ar), 7.45 (d, J = 5.3 Hz, 2H, Ar), 7.48 (s, 1H, NH_2), 8.08 (s, 1H, NH_2), 11.18 (s, 1H, NH). ^{13}C NMR (75.5 MHz, DMSO-d_6): 34.5 (S-CH_2), 115.9 (C-Ar), 116.2 (C-Ar), 129.7 (C-Ar), 131.5 (C-Ar), 131.6 (C-S), 141.4 (C=N), 162.6 (C-Ar), 177.8 (C=S). HRMS (ESI): 244.0405 $[M + H]^+$. Anal. Calcd for $C_9H_{10}FN_3S_2$: C, 44.43; H, 4.14; N, 17.27; S, 26.35; found: C, 44.31; H, 4.11; N, 17.33; S, 26.31.

4.2.3. 2-{2-[(4-bromophenyl)thio]ethylidene} thiosemicarbazone (**6**)

Crystallization from toluene/hexane 7:3, afforded yellow crystals, yield = 37%. Mp (ºC): 104-106. IR (KBr): 1594 (C=N), 3239 (NH), 3387 (NH_2) cm^{-1}. ^{1}H NMR (300 MHz, DMSO-d_6): 3.74 (d, 2H, S-CH_2), 7.17 (t, 2H, Ar), 7.31 (t, 1H, N=CH), 7.42 (dd, 2H, Ar), 7.49 (s, 1H, NH_2), 8.09 (s, 1H, NH_2), 11.18 (s, 1H, NH). ^{13}C NMR (75.5 MHz, DMSO-d_6): 33.3 (S-CH_2), 118.9 (C-Ar), 130.1 (C-Ar), 131.7 (C-Ar), 133.7 (C-Ar), 134.2 (C-Ar), 135.4 (C-Ar), 140.9 (C=N), 177.8 (C=S). HRMS (ESI): 303.9504 $[M + H]^+$. Anal. Calcd for $C_9H_{10}BrN_3S_2$: C, 35.53; H, 3.31; N, 13.81; S, 21.08; found: C, 35.62; H, 3.38; N, 13.85; S, 20.92.

4.2.4. 2-{2-[(4-methoxyphenyl)thio]ethylidene} thiosemicarbazone (**7**)

Crystallization from toluene/hexane 7:3, afforded orange crystals, yield = 30%. Mp (ºC): 124. IR (KBr): 1598 (C=N), 3255 (NH), 3404 (NH_2) cm^{-1}. ^{1}H NMR (300 MHz, DMSO-d_6): δ 3.64 (d, J = 6.0 Hz, 2H, S-CH_2), 3.73 (s, 3H, CH_3), 6.90 (d, J = 8.8 Hz, 2H, Ar), 7.31 – 7.37 (m, 3H, Ar, N=CH), 7.41 (s, 1H, NH_2), 8.05 (s, 1H, NH_2), 11.16 (s, 1H, NH). ^{13}C NMR (75.5 MHz, DMSO-d_6): 35.7 (S-CH_2), 55.2 (O-CH_3), 114.7 (C-Ar), 124.0 (C-Ar), 132.5 (C-S), 158.6 (C-Ar), 142.1 (C=N), 177.7 (C=S). HRMS (ESI): 256.0612 $[M + H]^+$.

Anal. Calcd for $C_{10}H_{13}N_3OS_2$: C, 47.04; H, 5.13; N, 16.46; S, 25.11; found: C, 47.34; H, 5.55; N, 16.23; S, 25.21.

4.2.5. 2-{2-[(2-methylphenyl)thio]ethylidene} thiosemicarbazone (**8**)

Crystallization from toluene/hexane 7:3, afforded white crystals, yield = 33%. Mp (ºC): 104-105. IR (KBr): 1599 (C=N), 3260 (NH), 3375 (NH_2) cm^{-1}. ^1H NMR (400 MHz, DMSO-d_6) δ 2.26 (s, 3H, CH_3), 3.74 (d, *J* = 6.0 Hz, 2H, S-CH_2), 7.10 (td, *J* = 1.3, 7.3 Hz, 1H, Ar), 7.15 (d, *J* = 5.8 Hz, 1H, Ar), 7.17 (t, *J* = 7.0 Hz, 1H, Ar), 7.31 (t, *J* = 6.0 Hz, 1H, HC=N), 7.38 (d, *J* = 6.5 Hz, 1H, Ar), 7.52 (s, 1H, NH_2), 7.93 (s, 1H, NH_2), 11.12 (s, 1H, NH). ^{13}C NMR (101 MHz, DMSO-d_6) δ 20.3 (CH_3), 33.7 (S-CH_2), 126.4 (C-Ar), 127.0 (C-Ar), 128.4 (C-Ar), 130.5 (C-Ar), 134.2 (C-Ar), 137.0 (C-Ar), 142.0 (C=N), 178.3 (C=S). HRMS (ESI): 240.0663 $[M + H]^+$. Anal. Calcd for $C_{10}H_{13}N_3S_2$: C, 50.18; H, 5.47; N, 17.56; S, 26.79; found: C, 50.23; H, 5.51; N, 17.46; S, 26.64.

4.2.6. 2-{2-[(3-methylphenyl)thio]ethylidene} thiosemicarbazone (**9**)

Crystallization from toluene/hexane 7:3, afforded yellow crystals, yield = 32%. Mp (ºC): 118-119. IR (KBr): 1604 (C=N), 3266 (NH), 3422 (NH_2) cm^{-1}. ^1H NMR (400 MHz, DMSO-d_6): 2.26 (3H, CH_3), 3.76 (d, *J* = 5.7 Hz, 2H, S-CH_2), 7.00 (d, *J* = 6.6 Hz, 1H, Ar), 7.24 – 7.10 (m, 3H, Ar), 7.33 (t, *J* = 5.7 Hz, 1H, N=CH), 7.51 (s, 1H, NH_2), 8.07 (s, 1H, NH_2, 11.17 (s, 1H, NH). ^{13}C NMR (100 MHz, Chloroform-*d*): 21.5 (CH_3), 35.8 (S-CH_2), 128.3 (C-Ar), 128.4 (C-Ar), 129.1 (C-Ar), 131.9 (C-Ar), 133.5 (C-Ar), 139.1 (C-Ar), 142.5 (C=N), 178.7 (C=S). HRMS (ESI): 240.0638 $[M + H]^+$. Anal. Calcd for $C_{10}H_{13}N_3S_2$: C, 50.18; H, 5.47; N, 17.56; S, 26.79; found: C, 50.12; H, 5.49; N, 17.46; S, 26.88.

4.2.7. 2-{2-[(4-methylphenyl)thio]ethylidene} thiosemicarbazone (**10**)

Crystallization from toluene/hexane 7:3, afforded yellow crystals, yield = 36%. Mp (ºC): 99-101. IR (KBr): 1602 (C=N), 3261 (NH), 3412 (NH_2).cm^{-1}. ^1H NMR (300 MHz, DMSO-d_6): 2.25 (3H, CH_3), 3.72 (d, 2H, S-CH_2), 7.19 (dd, 4H, Ar), 7.31 (t, 1H, N=CH), 7.51 (s, 1H, NH_2), 8.08 (s, 1H, NH_2), 11.18 (s, 1H, NH). ^{13}C NMR (75.5 MHz, DMSO-d_6): 20.6 (CH_3), 34.1 (S-CH_2), 129.2 (C-Ar), 129.7 (C-Ar), 130.7 (C-Ar), 135.8 (C-S), 141.8 (C=N), 177.8 (C=S). HRMS (ESI): 240.0643 $[M + H]^+$. Anal. Calcd for $C_{10}H_{13}N_3S_2$: C, 50.18; H, 5.47; N, 17.56; S, 26.79; found: C, 50.21; H, 5.43; N, 17.42; S, 26.86.

4.2.8. 2-{2-[(2,5-dimethylphenyl)thio]ethylidene} thiosemicarbazone (**11**)

Crystallization from toluene/hexane 7:3, afforded yellow crystals, yield = 35%. Mp (ºC): 119-120. IR (KBr): 1243 (C=S), 1597 (C=N), 3252 (NH), 3377 (NH_2) cm^{-1}. 1H NMR (300 MHz, DMSO-d_6) δ 2.24 (s, 6H, CH_3), 3.76 (d, J = 5.7 Hz, 2H, S-CH_2), 6.91 (d, J = 7.4 Hz, 1H, Ar), 7.08 (d, J = 7.5 Hz, 1H, Ar), 7.23 (s, 1H, Ar), 7.32 (t, J = 5.5 Hz, 1H, N=CH), 7.55 (s, 1H, NH_2), 8.11 (s, 1H, NH_2), 11.20 (s, 1H, NH). ^{13}C NMR (75.5 MHz, DMSO-d_6): 19.4 (CH_3), 20.5 (CH_3), 33.2 (S-CH_2), 126.6 (C-Ar), 128.3 (C-Ar), 128.4 (C-Ar), 129.9 (C-Ar), 133.4 (C-Ar), 135.6 (C-Ar), 141.3 (C=N), 177.9 (C=S). HRMS (ESI): 254.0823 $[M + H]^+$. Anal. Calcd for $C_{11}H_{15}N_3S_2$: C, 52.14; H, 5.97; N, 16.58; S, 25.31; found: C, 52.28; H, 6.08; N, 16.65; S, 25.41.

4.2.9. 2-{2-[(2-chlorophenyl)thio]ethylidene} thiosemicarbazone (**12**)

Crystallization from toluene/hexane 7:3, afforded yellow crystals, yield = 31%. Mp (ºC): 125-126. IR (KBr): 1601 (C=N), 3241 (NH), 3376 (NH_2) cm^{-1}. ^1H NMR (300 MHz, DMSO-d_6) δ 3.86 (d, J = 5.7 Hz, 2H, S-CH_2), 7.20 (t, J = 7.6 Hz, 1H, N=CH), 7.32 (t, J =

6.0 Hz, 2H, Ar), 7.46 (d, *J* = 7.8 Hz, 1H, Ar), 7.55 (d, *J* = 8.0 Hz, 1H, Ar), 7.67 (s, 1H, NH_2), 8.14 (s, 1H, NH_2), 11.24 (s, 1H, NH). ^{13}C NMR (75.5 MHz, DMSO-d_6): 32.5 (S-CH_2), 126.9 (C-Ar), 127.8 (C-Ar), 128.0 (C-Ar), 129.5 (C-Ar), 131.2 (C-Ar), 134.2 (C-Ar), 140.6 (C=N), 177.9 (C=S). HRMS (ESI): 260.0119 $[M + H]^+$. Anal. Calcd for $C_9H_{10}ClN_3S_2$: C, 41.61; H, 3.88; N, 16.18; S, 24.68; found: C, 41.41; H, 3.93; N, 16.25; S, 24.73.

4.2.10. 2-{2-[(3-chlorophenyl)thio]ethylidene} thiosemicarbazone (**13**)

Crystallization from toluene/hexane 7:3, afforded yellow crystals, yield = 32%. Mp (ºC): 111. IR (KBr): 1598 (C=N), 3245 (NH), 3439 (NH_2) cm^{-1}.^{1}H NMR (300 MHz, DMSO-d_6) δ 3.94 (d, *J* = 5.9 Hz, 2H, S-CH_2), 7.25 (d, *J* = 2.3 Hz, 1H, N=CH), 7.28 (d, *J* = 2.3 Hz, 1H, Ar), 7.32 (t, *J* = 5.9 Hz, 1H, Ar), 7.46 – 7.54 (m, 1H, Ar), 7.57 (d, *J* = 2.4 Hz, 1H, Ar), 8.22 (s, 1H, NH_2), 8.65 (s, 1H, NH_2), 11.28 (s, 1H, NH). ^{13}C NMR (75,5 MHz, DMSO-d_6): 32.4 (S-CH_2), 126.5 (C-Ar), 126.7 (C-Ar), 129.5 (C-Ar), 130.9 (C-Ar), 132.4 (C-Ar), 136.8 (C-Ar), 140.1 (C=N), 178.0 (C=S). HRMS (ESI): 260.0017 $[M + H]^+$. Anal. Calcd for $C_9H_{10}ClN_3S_2$: C, 41.61; H, 3.88; N, 16.18; S, 24.68; found: C, 41.55; H, 3.94; N, 16.27; S, 24.63.

4.2.11. 2-{2-[(4-chlorophenyl)thio]ethylidene} thiosemicarbazone (**14**)

Crystallization from toluene/hexane 7:3, afforded yellow crystals, yield = 38%. Mp (ºC): 133-135. IR (KBr): 1606 (C=N), 3249 (NH), 3411 (NH_2) cm^{-1}. ^{1}H NMR (400 MHz, DMSO-d_6) δ 3.75 (d, *J* = 6.0 Hz, 2H, S-CH_2), 7.27 (t, *J* = 6.0 Hz, 1H, N=CH), 7.32 (d, *J* = 8.7 Hz, 2H, Ar), 7.36 (d, *J* = 8.8 Hz, 2H, Ar), 7.56 (s, 1H, NH_2), 7.88 (s, 1H, NH_2), 11.09 (s, 1H, NH). ^{13}C NMR (75,5 MHz, DMSO-d_6): 34.0 (S-CH_2), 129.3 (C-Ar), 130.5 (C-Ar), 131.1 (C-Ar), 134.1 (C-Ar), 141.0 (C=N), 177.9 (C=S). HRMS (ESI): 260.0119 $[M + H]^+$.

Anal. Calcd for $C_9H_{10}ClN_3S_2$: C, 41.61; H, 3.88; N, 16.18; S, 24.68; found: C, 41.81; H, 3.94;N, 16.17; S, 24.69.

4.2.12. 2-{2-[(2,5-dichlorophenyl)thio]ethylidene} thiosemicarbazone (**15**)

Crystallization from toluene/hexane 7:3, afforded yellow crystals, yield = 36%. Mp (ºC): 149-150. IR (KBr): 1601 (C=N), 3241 (NH), 3402 (NH_2) cm^{-1}. ^1H NMR (300 MHz, DMSO-d_6) δ 3.94 (d, J = 5.9 Hz, 2H, S-CH_2), 7.25 (d, J = 2.3 Hz, 1H, Ar), 7.28 (d, J = 2.3 Hz, 1H, Ar), 7.32 (t, J = 5.9 Hz, 1H, N=CH), 7.47 (s, 1H, Ar), 8.22 (s, 1H, NH_2), 8.65 (s, 1H, NH_2), 11.28 (s, 1H, NH). ^{13}C NMR (75.5 MHz, DMSO-d_6): 32.4 (S-CH_2), 126.5 (C-Ar), 126.7 (C-Ar), 129.5 (C-Ar), 130.9 (C-Ar), 132.4 (C-Ar), 136.8 (C-Ar), 140.1 (C=N), 178.0 (C=S).

HRMS (ESI): 293.8745 $[M + H]^+$. Anal. Calcd for $C_9H_9Cl_2N_3S_2$: C, 36.74; H, 3.08; N, 14.28; S, 21.79; found: C, 36.78; H, 3.17; N, 14.31; S, 21.84.

4.3. General procedure for the synthesis of 1,3-thiazoles (**16**-**26**)

Example for compound (**16**): Thiosemicarbazone (**4**) (0.45 g, 2 mmol) was dissolved in 2-propanol (10 mL), and then 2-bromoacetophenone (0.48 g, 2.4 mmol) and calcium carbonate (0.24 g, 2.4 mmol) were added to a glass tube. The tube was placed in an ultrasonic bath (40 MHz, 180 V) and irradiated for 60 min at r.t. Hexane was added, and the mixture was cooled in a freezer overnight. The precipitate was filtered off and washed with hexane and then dried in a desiccator under vacuum. An additional amount of the desired compound was obtained from the filtrate after cooling. Pure products were obtained after recrystallization using the solvent system detailed below for each compound.

4.3.1. 2-{2-[2-(phenylthio)ethylidene]hydrazinyl}-4-phenyl-1,3-thiazole (**16**)

Crystallization from toluene/hexane 7:3, afforded brown crystals, yield = 72%. Mp (ºC): 148-149. IR (KBr): 1581 (C=N), 1611 (C=N), 3089 (N-H) cm^{-1}. ^{1}H NMR (300 MHz, DMSO-d_6) δ 3.85 (d, *J* = 5.9 Hz, 2H, S-CH_2), 5.89 (bs, 1H, NH), 7.19 (t, *J* = 7.1 Hz, 2H, Ar), 7.27 (s, 1H, Ar), 7.32 (t, *J* = 6.4 Hz, 2H, Ar), 7.35 – 7.49 (m, 5H, Ar, CH), 7.79 (d, *J* = 7.4 Hz, 2H, Ar). ^{13}C NMR (75.5 MHz, DMSO-d_6): 33.8 (S-CH_3), 103.7 (S-CH), 125.7 (C-Ar), 126.2 (C-Ar), 127.8 (C-Ar), 128.3 (C-Ar), 128.6 (C-Ar), 129.0 (C-Ar), 133.8 (C-Ar), 134.7 (S-C), 141.6 (C-Ar), 148.9 (N=CH), 168.2 (N=C). HRMS (ESI): 326.0610 $[M + H]^+$. Anal. Calcd for $C_{17}H_{15}N_3S_2$: C, 62.74; H, 4.65; N, 12.91; S, 19.70; found: C, 62.72; H, 4.68; N, 12.96; S, 19.63.

4.3.2. 2-{2-[2-(phenylthio)ethylidene]hydrazineyl}-4-(p-tolyl)-1,3-thiazole (**17**)

Crystallization from toluene/hexane 7:3, afforded yellow crystals, yield = 68%. Mp (ºC): 148-149. IR (KBr): 1568 (C=N), 1625 (C=N), 3083 (N-H) cm^{-1}. ^{1}H NMR (400 MHz, DMSO-d_6) δ 2.27 (s, 3H, CH_3), 3.79 (d, *J* = 6.0 Hz, 2H, S-CH_2), 4.19 (s, 1H, NH), 7.11 (s, 1H, Ar), 7.18 (d, *J* = 8.4 Hz, 2H, Ar), 7.31 (t, *J* = 7.4 Hz, 1H, Ar), 7.36 (t, *J* = 6.4 Hz, 2H, Ar), 7.63 (d, *J* = 7.9 Hz, 3H, Ar), 7.76 (d, *J* = 8.0 Hz, 2H, Ar). ^{13}C NMR (75.5 MHz, DMSO-d_6): 20.8 (CH_3), 33.8 (S-CH_2), 102.6 (S-CH), 125.5 (C-Ar), 126.1 (C-Ar), 126.9 (C-Ar), 128.6 (C-Ar), 128.9 (C-Ar), 129.1 (C-Ar), 129.6 (C-Ar), 131.3 (C-Ar), 134.7 (S-C), 136.9 (C-Ar), 141.6 (C-Ar), 151.2 (N=CH), 168.0 (N=C). HRMS (ESI): 340.0950 $[M + H]^+$. Anal. Calcd for $C_{18}H_{17}N_3S_2$: C, 63.69; H, 5.05; N, 12.38; S, 18.89; found: C, 63.74; H, 5.15; N, 12.32; S, 18.91.

4.3.3. 2-{2-[2-(phenylthio)ethylidene]hydrazinyl}-4-(4-bromophenyl)-5-methyl-1,3-thiazole (**18**)

Crystallization from toluene/hexane 7:3, afforded yellow crystals, yield = 61%. Mp (ºC): 202. IR (KBr): 1608 (C=N), 3123 (N-H) cm^{-1}. ^{1}H NMR (300 MHz, DMSO-d_6): 2.35 (s, 3H, CH_3), 3.84 (d, *J* = 6.0 Hz, 2H, S-CH_2), 5.39 (bs, 1H, NH), 7.20 (t, *J* = 7.3 Hz, 1H, N=CH), 7.31 (d, *J* = 7.9 Hz, 2H, Ar), 7.32-7.37 (m, 5H, Ar, CH_2), 7.40 (d, *J* = 7.5 Hz, 2H, Ar). ^{13}C NMR (75.5 MHz, DMSO-d_6): 12.0 (CH_3), 33.6 (S-CH_2), 117.4 (S-CH), 120.6 (C-Ar), 126.0 (C-Ar), 128.4 (C-Ar), 128.9 (C-Ar), 130.0 (C-Ar), 131.2 (C-Ar), 134.6 (S-C), 141.9 (C-Ar), 151.2 (N=CH), 164.6 (N=C). HRMS (ESI): 416.9026 [M]. Anal. Calcd for $C_{18}H_{16}BrN_3S_2$: C, 51.68; H, 3.85; N, 10.04; S, 15.33; found: C, 51.74; H, 3.77; N, 10.13; S, 15.29

4.3.4. 2-{2-[2-(phenylthio)ethylidene]hydrazinyl}-4-(4-bromophenyl)-1,3-thiazole (**19**)

Crystallization from toluene/hexane 7:3, afforded yellow crystals, yield = 61%. Mp (ºC): 202. IR (KBr): 1608 (C=N), 3123 (N-H) cm^{-1}. ^{1}H NMR (400 MHz, DMSO-d_6) δ 3.79 (d, *J* = 5.9 Hz, 2H, S-CH_2), 4.22 (bs, 1H, NH), 7.17 (t, *J* = 7.3 Hz, 1H, N=CH), 7.25 (s, 1H, Ar), 7.29 (t, *J* = 7.8 Hz, 2H, Ar), 7.35 (t, *J* = 9.9 Hz, 1H, N=CH), 7.54 (d, *J* = 9.6 Hz, 1H, Ar), 7.60 (d, *J* = 8.1 Hz, 1H, Ar), 7.71 (d, *J* = 8.3 Hz, 2H, Ar), 7.81 (d, *J* = 9.2 Hz, 2H, Ar). ^{13}C NMR (75.5 MHz, DMSO-d_6): 22.5 (S-CH_2), 104.8 (S-CH), 120.5 (C-Ar), 121.5 (C-Ar), 128.0 (C-Ar), 128.2 (C-Ar), 129.0 (C-Ar), 129.4 (C-Ar), 131.9 (C-Ar), 132.0 (C-Ar), 132.5 (C-Ar), 132.7 (S-C), 141.9 (C-Ar), 151.2 (N=CH), 164.6 (N=C). HRMS (ESI): 405.9894 $[M + H]^+$. Anal. Calcd for $C_{17}H_{14}BrN_3S_2$: C, 50.50; H, 3.49; N, 10.39; S, 15.86; found: C, 50.54; H, 3.51; N, 10.33; S, 15.95.

4.3.5. 2-{2-[2-(phenylthio)ethylidene]hydrazinyl}-4-(4-fluorophenyl)-1,3-thiazole (**20**)

Crystallization from toluene/hexane 7:3, afforded brown crystals, yield = 63%. Mp (ºC): 228. IR (KBr): 1508 (C=C), 1614 (C=N), 3082 (N-H) cm^{-1}. ^{1}H NMR (400 MHz, DMSO-d_6) δ 3.84 (d, *J* = 5.9 Hz, 2H, S-CH_2), 5.16 (bs, 1H, NH), 7.21 (t, *J* = 8.4 Hz, 1H, Ar), 7.23 (s, 1H, Ar), 7.31 (t, *J* = 7.6 Hz, 2H, Ar), 7.35 (t, *J* = 6.0 Hz, 1H, N=CH), 7.40 (d, *J* = 7.8 Hz, 2H, Ar), 7.82 (d, *J* = 5.8 Hz, 2H, Ar), 7.84 (d, *J* = 5.9 Hz, 2H, Ar). ^{13}C NMR (101 MHz, DMSO-d_6) δ 33.8 (S-CH_2), 103.3 (S-CH), , 115.6 (C-Ar), 126.1 (C-Ar), 127.5 (C-Ar), 127.6 (C-Ar), 128.3 (C-Ar), 128.6 (C-Ar), 128.9 (C-Ar), 130.8 (C-Ar), 134.7 (S-C), 140.9 (C-Ar), 148.6 (C-Ar), 160.4 (C-Ar), 162.8 (C-Ar), 168.2 (N=C). HRMS (ESI): 344.0702 $[M + H]^+$. Anal. Calcd for $C_{17}H_{14}FN_3S_2$: C, 59.45; H, 4.11; N, 12.24; S, 18.67; found: C, 59.52; H, 4.19; N, 12.28; S, 18.74.

4.3.6. 2-{2-[2-(phenylthio)ethylidene]hydrazinyl}-4-(4-methoxyphenyl)-1,3-thiazole (**21**)

Crystallization from toluene/hexane 7:3, afforded yellow crystals, yield = 62%. Mp (ºC): 187. IR (KBr): 1530 (C=N), 1606 (C=N), 3203 (N-H) cm^{-1}. ^{1}H NMR (400 MHz, DMSO-d_6) δ 3.75 (s, 3H, CH_3), 3.83 (d, *J* = 6.3 Hz, 2H, S-CH_2), 5.00 (bs, 1H, NH), 6.94 (d, *J* = 8.3 Hz, 1H, Ar), 6.99 (d, *J* = 8.4 Hz, 1H, Ar), 7.07 (s, 1H, Ar), 7.18 (t, *J* = 7.4 Hz, 1H, Ar), 7.30 (t, *J* = 7.6 Hz, 2H, Ar), 7.34 (t, *J* = 5.9 Hz, 1H, N=CH), 7.39 (d, *J* = 7.8 Hz, 1H, Ar), 7.43 (d, *J* = 8.8 Hz, 1H, Ar), 7.70 (d, *J* = 8.3 Hz, 2H, Ar). ^{13}C NMR (75.5 MHz, DMSO-d_6): 33.8 (S-CH_2), 55.2 (CH_3), 101.4 (S-CH), 113.9 (C-Ar), 126.1 (C-Ar), 126.9 (C-Ar), 128.6 (C-Ar), 128.9 (C-Ar), 134.7 (S-C), 141.2 (C-Ar), 148.9 (N=CH), 168.9 (N=C). HRMS (ESI): 356.0944 $[M + H]^+$. Anal. Calcd for $C_{18}H_{17}N_3OS_2$: C, 60.82; H, 4.82; N, 11.82; S, 18.04; found: C, 60.86; H, 4.79; N, 11.95; S, 18.16.

4.3.7. 2-{2-[2-(phenylthio)ethylidene]hydrazinyl}-4-(4-chlorophenyl)-1,3-thiazole (**22**)

Crystallization from toluene/hexane 7:3, afforded brown crystals, yield = 68%. Mp (ºC): 226. IR (KBr): 1581 (C=N), 1628 (C=N), 3147 (N-H) cm^{-1}. ^{1}H NMR (300 MHz, DMSO-d_6): 3.84 (d, 2H, *J* = 5.9 Hz, S-CH_2), 5.84 (bs, 1H, NH), 7.19 (t, 1H, *J* = 7.4 Hz, N=CH), 7.21 (s, 1H, Ar), 7.28-7.49 (m, 5H, Ar) 7.84 (dd, 4H, *J* = 7.8, 3.5 Hz, Ar). ^{13}C NMR (75.5 MHz, DMSO-d_6): 34.2 (S-CH_2), 104.7 (S-CH), 126.5 (C-Ar), 127.6 (C-Ar), 129.1 (C-Ar), 129.4 (C-Ar), 132.4 (C-Ar), 133.7 (S-C), 135.1 (C-Ar), 141.2 (C-Ar), 149.2 (N=CH), 168.6 (N=C). HRMS (ESI): 360.0282 $[M + H]^+$. Anal. Calcd for $C_{17}H_{14}ClN_3S_2$: C, 56.74; H, 3.92; N, 11.68; S, 17.82; found: C, 56.83; H, 4.01; N, 11.73; S, 17.74.

4.3.8. 2-{2-[2-(phenylthio)ethylidene]hydrazinyl}-4-(2,4-dichlorophenyl)-1,3-thiazole (**23**)

Crystallization from toluene/hexane 7:3, afforded yellow crystals, yield = 62%. Mp (ºC): 211. IR (KBr): 1549 (C=N), 1621 (C=N), 3129 (N-H) cm^{-1}. ^{1}H NMR (300 MHz, DMSO-d_6): 3.84 (d, 2H, *J* = 6.0 Hz, S-CH_2), 4.99 (bs, 1H, NH), 7.18 (t, 1H, *J* = 7.0 Hz, N=CH), 7.28-7.83 (m, 9H, Ar). ^{13}C NMR (75.5 MHz, DMSO-d_6): 34.2 (S-CH_2), 109.4 (S-CH), 126.5 (C-Ar), 127.9 (C-Ar), 129.0 (C-Ar), 129.4 (C-Ar), 130.1 (C-Ar), 132.6 (C-Ar), 135.1 (C-Ar), 141.2 (C-Ar), 165.5 (C=N), 167.7 (S-C=N). HRMS (ESI): 393.9929 $[M + H]^+$. Anal. Calcd for $C_{17}H_{13}Cl_2N_3S_2$: C, 51.78; H, 3.32; N, 10.66; S, 16.26; found: C, 51.86; H, 3.38; N, 10.59; S, 16.32.

4.3.9. 2-{2-[2-(phenylthio)ethylidene]hydrazinyl}-4-(3,4-dichlorophenyl)-1,3-thiazole (**24**)

Crystallization from toluene/hexane 7:3, afforded yellow crystals, yield = 61%. Mp (ºC): 217. IR (KBr): 1578 (C=N), 1614 (C=N), 3087 (N-H) cm^{-1}. ^{1}H NMR (300 MHz, DMSO-

d_6): 3.84 (d, 2H, *J* = 6.0 Hz, S-CH_2), 5.08 (bs, 1H, NH), 7.19 (t, 1H, *J* = 7.2 Hz, N=CH), 7.28-7.41 (m, 4H, Ar, CH) 7.48 (s, 1H, N=CH), 7.64 (d, 2H, *J* = 8.4 Hz, Ar), 7.79 (d, 2H, *J* = 8.4 Hz, Ar). ^{13}C NMR (75.5 MHz, DMSO-d_6): 33.8 (S-CH_2), 105.7 (S-CH), 125.5 (C-Ar), 126.1 (C-Ar), 127.1 (C-Ar), 128.7 (C-Ar), 129.0 (C-Ar), 129.6 (C-Ar), 130.8 (C-Ar), 131.4 (C-Ar), 134.7 (S-C), 135.1 (C-Ar), 140.8 (C-Ar), 147.6 (N=CH), 168.2 (N=C). HRMS (ESI): 394.0009 $[M + H]^+$. Anal. Calcd for $C_{17}H_{13}Cl_2N_3S_2$: C, 51.78; H, 3.32; N, 10.66; S, 16.26; found: C, 51.72; H, 3.38; N, 10.71; S, 16.32.

4.3.10. 2-{2-[2-(phenylthio)ethylidene]hydrazinyl}-4-(3-nitrophenyl)-1,3-thiazole (**25**)

Crystallization from toluene/hexane 7:3, afforded yellow crystals, yield = 59%. Mp (ºC): 226. IR (KBr): 1354 (NO_2), 1524 (C=N), 1639 (C=N), 3135 (N-H) cm^{-1}. ^{1}H NMR (300 MHz, DMSO-d_6): 3.81 (d, 2H, S-CH_2), 4.02 (bs, 1H, NH), 7.19 (t, 1H, *J* = 7.2 Hz, N=CH), 7.29-7.42 (m, 4H, Ar, CH), 7.58 (s, 1H, N=CH), 7.68 (t, 1H, *J* = 8.0 Hz, N=CH), 8.11-8.60 (m, 4H, Ar). ^{13}C NMR (75.5 MHz, DMSO-d_6): 34.3 (S-CH_2), 103.3 (S-CH), 119.9 (C-Ar), 126.0 (C-Ar), 126.6 (C-Ar), 128.1 (C-Ar), 129.1 (C-Ar), 129.4 (C-Ar), 129.6 (C-Ar), 131.4 (C-Ar), 135.1 (C-Ar), 137.7 (S-C), 142.3 (C-Ar), 149.0 (N=CH), 168.6 (N=C). HRMS (ESI): 371.0558 $[M + H]^+$. Anal. Calcd for $C_{17}H_{14}N_4O_2S_2$: C, 55.12; H, 3.81; N, 15.12; S, 17.31; found: C, 55.02; H, 3.87; N, 15.19; S, 17.39.

4.3.11. 2-{2-[2-(phenylthio)ethylidene]hydrazinyl}-4-(4-nitrophenyl)-1,3-thiazole (**26**)

Crystallization from toluene/hexane 7:3, afforded orange crystals, yield = 60%. Mp (ºC): 220. IR (KBr): 1339 (NO_2), 1596 (C=N), 3048 (N-H) cm^{-1}. ^{1}H NMR (400 MHz, DMSO-d_6) δ 3.84 (d, *J* = 5.9 Hz, 2H, S-CH_2), 6.04 (bs, 1H, NH), 7.19 (t, *J* = 7.3 Hz, 1H, Ar), 7.31 (t, *J* = 7.1 Hz, 2H, Ar), 7.35 (t, *J* = 5.8 Hz, 1H, N=CH), 7.40 (d, *J* = 7.7 Hz, 2H, Ar), 7.63 (s, 1H,

Ar), 8.05 (d, *J* = 8.4 Hz, 2H, Ar), 8.24 (d, *J* = 8.5 Hz, 2H, Ar).^{13}C NMR (101 MHz, DMSO-d_6): 34.3 (S-CH_2), 108.8 (S-CH), 124.5 (C-Ar), 126.6 (C-Ar), 126.7 (C-Ar), 129.1 (C-Ar), 129.4 (C-Ar), 135.2 (C-Ar), 141.0 (C-Ar), 141.3 (C-Ar), 146.3 (C-Ar), 146.6 (S-C), 148.7 (N=CH), 168.9 (N=C). HRMS (ESI): 371.0692 $[M + H]^+$. Anal. Calcd for $C_{17}H_{14}N_4O_2S_2$: C, 55.12; H, 3.81; N, 15.12; S, 17.31; found: C, 55.09; H, 3.94; N, 15.21; S, 17.25.

4.4.Biology

4.4.1. Cruzain inhibition

Cruzain activity was measured by monitoring the cleavage of the fluorescent substrate Z-Phe-Arg-aminomethylcoumarin (Z-FR-AMC) in a Synergy 2 (Biotek) fluorimeter at the Centre for Flow Cytometry Fluorimetry at the Department of Biochemistry and Immunology (UFMG), as previously reported[40]. All assays were performed in a buffer solution of 0.1 M sodium acetate pH 5.5 in the presence of 0.1 mM beta-mercaptoethanol, 0.01% Triton X-100, 0.5 nM cruzain and 2.5 µM of substrate (Km = 1 µM). Initially, the compounds were pre-incubated in a solution containing the enzyme. After 10 min of incubation, the substrate was added. The initial screening with 100 µM of inhibitor was performed in at least five independent experiments, each in triplicate, monitored for 5 min. Enzymatic activity was calculated based on comparison with a DMSO control from the initial rates of reaction. IC_{50} values represent an average of two independent experiments, each involving at least seven compound concentrations in triplicate. IC_{50} curves were determined with GraphPad Prism.

4.4.2. Animals

Female BALB/c mice (6–8 weeks old) were supplied by the animal breeding facility at Centro de Pesquisas Gonçalo Moniz (Fundação Oswaldo Cruz, Bahia, Brazil) and maintained in sterilized cages under a controlled environment, receiving a balanced diet for rodents and water ad libitum. All experiments were carried out following the recommendations of the Ethical Issues Guidelines and were approved by the local Animal Ethics Committee.

4.4.3. Parasites

Epimastigotes of *T. cruzi* (Y strain) were maintained at 26 °C in LIT medium (Liver Infusion Tryptose) supplemented with 10% fetal bovine serum (FBS) (Cultilab, Campinas, SP, Brazil), 1% hemin (Sigma Co, St. Louis, MO, USA), 1% R9 medium (Sigma Co), and 50 µg/mL gentamycin (Novafarma, Anápolis, GO, Brazil). Bloodstream trypomastigote forms of *T. cruzi* were obtained from supernatants of LLC-MK_2 cells previously infected and maintained in RPMI-1640 medium (Sigma Co) supplemented with 10% FBS and 50 µg/mL gentamycin at 37 °C and 5% CO_2.

4.4.4. Cytotoxicity to mouse splenocytes

BALB/c mouse splenocytes were placed in 96-well plates at a cell density of $5x10^6$ cells/well in RPMI-1640 medium supplemented with 10% of FBS and 50 µg mL^{-1} of gentamycin. Each test inhibitor was used in at least three concentrations (1.0, 10, and 100 µg/mL) in triplicate. To each well, an aliquot of test inhibitor suspended in DMSO was added. Negative (untreated) and positive (saponin) controls were carried out in every plate. The plate was incubated for 24 h at 37 ºC and 5% CO_2. After incubation, 1.0 µCi of ^{3}H-thymidine (Perkin Elmer, Waltham, USA) was added to each well, and the plate was

returned to the incubator. The plate was then transferred to a beta-radiation counter (Multilabel Reader, Finland), and the per cent of ^{3}H-thymidine was determined. Cell viability was measured as the per cent of ^{3}H-thymidine incorporation for treated cells in comparison to untreated cells. The highest non-toxic concentration was estimated using the average of the duplicates.

4.4.5. Antiproliferative activity for epimastigotes

Epimastigotes (Dm28c) were counted in a hemocytometer and then dispensed into 96-well plates at a cell density of 10^6 cells/well. Test inhibitors dissolved in DMSO were diluted to five different concentrations (1.23, 3.70, 11.11, 33.33, and 100 μg/mL) and added to the respective wells in triplicate. The plate was incubated for five days at 26 °C, and aliquots of each well were collected. The number of viable parasites was counted in a Neubauer chamber and compared to untreated parasite culture. IC_{50} values were calculated using non-linear regression on Prism 4.0 GraphPad software. This experiment was performed in duplicate, and Benznidazole (LAFEPE, Brazil) was used as the reference inhibitor.

4.4.6. Anti-T. cruzi activity (trypomastigotes)

Trypomastigotes collected from the supernatant of LLC-MK_2 cells were dispensed into 96-well plates at a cell density of $4x10^5$ cells/well in duplicate. Test inhibitors dissolved in DMSO were diluted to five different concentrations (1.23, 3.70, 11.11, 33.33, and 100 μg/mL) and added into their respective wells, and the plates were incubated for 24 h at 37 ºC and 5% of CO_2. The final DMSO concentration was 1%. Aliquots of each well were collected, and the number of viable parasites, based on parasite motility, was assessed in a Neubauer chamber. The percentage of inhibition was calculated concerning untreated

cultures. IC_{50} calculation was also carried out using non-linear regression with Prism 4.0 GraphPad software. Benznidazole was used as the reference drug.

4.4.7. In vitro T. cruzi infection assay

Peritoneal exudate macrophages were obtained by washing, with cold RPMI medium, the peritoneal cavity of BALB/c mice four-five days after the injection of 3% thioglycolate (Sigma Co) in saline (1.5 mL per mice). Then, the cells were plated at a cell density of $2x10^5$ cells/well in 24-well plates with sterile coverslips on the bottom in RPMI supplemented with 10% FBS and incubated for 24 h. Cells were then infected with trypomastigotes at a ratio of 10 parasites per macrophage for 2 h. Free trypomastigotes were removed by successive washes using saline solution. Cultures were incubated in complete medium alone or with compounds **17**, **18**, **22**, and **26** in different concentrations for 6 h. The medium was replaced with fresh medium, and the plate was incubated for three days. Cells were fixed in absolute alcohol, and the percentage of infected macrophages and the mean number of amastigotes/100 macrophages was determined by manual counting after Giemsa staining using an optical microscope (Olympus, Tokyo, Japan). The percentage of infected macrophages and the relative number of amastigotes per macrophage was determined by counting 100 cells per slide. IC_{50} calculation was also carried out using non-linear regression with Prism 4.0 GraphPad software. This experiment was performed twice, and benznidazole was used as a positive control.

4.4.8. Trypomastigote invasion

Peritoneal exudate macrophages (10^5 cells) were plated onto 13-mm glass coverslips in 24-well plates and kept for 24 h at 37 °C and 5% CO_2. The plate was washed with saline

solution, and then trypomastigotes were added at a cell density of $1.25x10^7$, along with the addition of test inhibitor (at 50 µM). Amphotericin B was used as the reference inhibitor. The plate was incubated for 2 h at 37 °C and 5% CO_2, followed by five washes with saline solution to remove extracellular trypomastigotes. Plates were maintained in RPMI medium supplemented with 10% FBS at 37 °C for 2 h. The number of infected cells was counted by optical microscopy using a standard Giemsa stain.

4.4.9. Flow cytometry analysis

Trypomastigotes (4×10^5 cells/mL) were resuspended in RPMI-1640 medium and treated with compounds **06**, **09**, **11**, **16**-**18**, **22**, and **23** (0.25 and 1.1 mM) for 24 h at 37 ^oC with 5% CO_2. Parasites were labelled with propidium iodide (PI) and annexin V using the annexin V-FITC apoptosis detection kit (Ebioscience, San Diego, USA) according to the manufacturer instructions. The experiment was performed using a BD Calibur flow cytometer (San Jose, USA) by acquiring at least 50,000 events, and data were analyzed by FlowJo software (Tree Star, Inc., San Carlos, USA). Two independent experiments, in duplicate, were performed.

4.4.10. Electron microscopy analysis

Trypomastigotes (3×10^7 cells/well) were incubated for 24 h at 37 °C in complete medium alone or with compound **18** (3 µM). After incubation, parasites were fixed in 2.5% glutaraldehyde (Electron Microscopy Sciences, Hatfield, PA) in 0.1 M sodium cacodylate buffer, pH 7.4, washed in the same buffer and then treated with a 1.0% solution of osmium tetroxide containing 0.8% potassium ferrocyanide (Sigma Co) for 1 h in the dark. Cells were dehydrated in an acetone series and infiltrated in polybed epoxy resin (Polysciences,

Warrington, PA). Ultrathin sections on copper grids were contrasted with uranyl acetate and lead citrate. The ultrastructure analysis was performed using a transmission electron microscope (Jeol JEM 1230).

4.4.11. Statistical analyses

To determine the statistical significance of each group in the *in vitro* experiments, the one-way ANOVA test and the Bonferroni correction for multiple comparisons were used. A *P* value < 0.05 was considered significant. The data are representative of at least two, or three experiments run in triplicate.

Acknowledgements

The authors are thankful to Centro de Citometria e Fluorimetria of UFMG / FAPEMIG for allowing the use of the fluorimeter, Department of Chemistry at the Federal University of Pernambuco (UFPE) for recording the NMR (^{1}H and ^{13}C) and IR spectra and the elemental analysis of all compounds and CETENE for the HRMS ESI-TOF experiments. MVOC is thankful to CNPq (grant number 427078/2016-4) and FACEPE (grant number APQ-0289-4.03/13 and APQ-0350-4.03/18) for financial support to develop this research.

References

[1] A.C. Aufderheide, W. Salo, M. Madden, J. Streitz, J. Buikstra, F. Guhl, B. Arriaza, C. Renier, L.E. Wittmers, G. Fornaciari, M. Allison, A 9,000-year record of Chagas' disease., Proc. Natl. Acad. Sci. U. S. A. 101 (2004) 2034–9. doi:10.1073/pnas.0307312101.

[2] P.J. Hotez, M.E. Bottazzi, C. Franco-Paredes, S.K. Ault, M.R. Periago, The neglected tropical diseases of Latin America and the Caribbean: a review of disease burden and distribution and a roadmap for control and elimination., PLoS Negl. Trop. Dis. 2 (2008) e300. doi:10.1371/journal.pntd.0000300.

[3] B.Y. Lee, K.M. Bacon, M.E. Bottazzi, P.J. Hotez, Global economic burden of Chagas disease: a computational simulation model., Lancet. Infect. Dis. 13 (2013) 342–8. doi:10.1016/S1473-3099(13)70002-1.

[4] R.L. Tarleton, R. Reithinger, J.A. Urbina, U. Kitron, R.E. Gürtler, The challenges of Chagas Disease-- grim outlook or glimmer of hope., PLoS Med. 4 (2007) e332. doi:10.1371/journal.pmed.0040332.

[5] WHO, Chagas disease (American trypanosomiasis), WHO. (2018).

[6] J. a. Urbina, Recent Clinical Trials for the Etiological Treatment of Chronic Chagas Disease: Advances, Challenges and Perspectives, J. Eukaryot. Microbiol. 62 (2015) 149–156. doi:10.1111/jeu.12184.

[7] M.-J. Pinazo, L. Guerrero, E. Posada, E. Rodríguez, D. Soy, J. Gascon, Benznidazole-related adverse drug reactions and their relationship to serum drug concentrations in patients with chronic chagas disease., Antimicrob. Agents Chemother. 57 (2013) 390–5. doi:10.1128/AAC.01401-12.

[8] D.H. Molyneux, L. Savioli, D. Engels, Neglected tropical diseases: progress towards

addressing the chronic pandemic, Lancet. 389 (2017) 312–325. doi:10.1016/S0140-6736(16)30171-4.

[9] J.A. Urbina, R. Docampo, Specific chemotherapy of Chagas disease: controversies and advances, Trends Parasitol. 19 (2003) 495–501. doi:10.1016/j.pt.2003.09.001.

[10] J. Urbina, Chemotherapy of Chagas Disease, Curr. Pharm. Des. 8 (2002) 287–295. doi:10.2174/1381612023396177.

[11] J.R. Cançado, Criteria of Chagas disease cure, Mem. Inst. Oswaldo Cruz. 94 (1999) 331–335. doi:10.1590/S0074-02761999000700064.

[12] A.L. Ribeiro, M.P. Nunes, M.M. Teixeira, M.O.C. Rocha, Diagnosis and management of Chagas disease and cardiomyopathy, Nat. Rev. Cardiol. 9 (2012) 576–589. doi:10.1038/nrcardio.2012.109.

[13] J. McKerrow, Cysteine protease inhibitors as chemotherapy for parasitic infections, Bioorg. Med. Chem. 7 (1999) 639–644. doi:10.1016/S0968-0896(99)00008-5.

[14] A.E. Eakin, M.E. McGrath, J.H. McKerrow, R.J. Fletterick, C.S. Craik, Production of crystallizable cruzain, the major cysteine protease from Trypanosoma cruzi., J. Biol. Chem. 268 (1993) 6115–8. http://www.ncbi.nlm.nih.gov/pubmed/8454586 (accessed May 24, 2013).

[15] J.H. McKerrow, M.E. McGrath, J.C. Engel, The cysteine protease of Trypanosoma cruzi as a model for antiparasite drug design, Parasitol. Today. 11 (1995) 279–282. doi:10.1016/0169-4758(95)80039-5.

[16] M.E. McGrath, A.E. Eakin, J.C. Engel, J.H. McKerrow, C.S. Craik, R.J. Fletterick, The crystal structure of cruzain: a therapeutic target for Chagas' disease., J. Mol. Biol. 247 (1995) 251–9. doi:10.1006/jmbi.1994.0137.

[17] M. Ndao, C. Beaulieu, W.C. Black, E. Isabel, F. Vasquez-Camargo, M. Nath-

Chowdhury, F. Massé, C. Mellon, N. Methot, D.A. Nicoll-Griffith, Reversible cysteine protease inhibitors show promise for a Chagas disease cure., Antimicrob. Agents Chemother. 58 (2014) 1167–78. doi:10.1128/AAC.01855-13.

[18] G. Harth, N. Andrews, A.A. Mills, J.C. Engel, R. Smith, J.H. McKerrow, Peptide-fluoromethyl ketones arrest intracellular replication and intercellular transmission of Trypanosoma cruzi, Mol. Biochem. Parasitol. 58 (1993) 17–24. doi:10.1016/0166-6851(93)90086-D.

[19] J.J. Cazzulo, Proteinases of Trypanosoma cruzi: patential targets for the chemotherapy of Changas desease., Curr. Top. Med. Chem. 2 (2002) 1261–71. http://www.ncbi.nlm.nih.gov/pubmed/12171584 (accessed November 14, 2013).

[20] A. Ayati, S. Emami, A. Asadipour, A. Shafiee, A. Foroumadi, Recent applications of 1,3-thiazole core structure in the identification of new lead compounds and drug discovery, Eur. J. Med. Chem. 97 (2015) 699–718. doi:10.1016/j.ejmech.2014.08.012.

[21] G. Álvarez, J. Martínez, J. Varela, E. Birriel, E. Cruces, M. Gabay, S.M. Leal, P. Escobar, B. Aguirre-López, N. Cabrera, M. Tuena de Gómez-Puyou, A. Gómez Puyou, R. Pérez-Montfort, G. Yaluff, S. Torres, E. Serna, N. Vera de Bilbao, M. González, H. Cerecetto, Development of bis-thiazoles as inhibitors of triosephosphate isomerase from Trypanosoma cruzi. Identification of new non-mutagenic agents that are active in vivo, Eur. J. Med. Chem. 100 (2015) 246–256. doi:10.1016/j.ejmech.2015.06.018.

[22] G. Álvarez, J. Varela, E. Cruces, M. Fernández, M. Gabay, S.M. Leal, P. Escobar, L. Sanabria, E. Serna, S. Torres, S.J. Figueredo Thiel, G. Yaluff, N.I. Vera de Bilbao, H. Cerecetto, M. González, Identification of a new amide-containing thiazole as a drug

candidate for treatment of Chagas' disease., Antimicrob. Agents Chemother. 59 (2015) 1398–404. doi:10.1128/AAC.03814-14.

[23] M.V. de O. Cardoso, L.R.P. de Siqueira, E.B. da Silva, L.B. Costa, M.Z. Hernandes, M.M. Rabello, R.S. Ferreira, L.F. da Cruz, D.R.M. Moreira, V.R.A. Pereira, M.C.A.B. de Castro, P. V. Bernhardt, A.C.L. Leite, 2-Pyridyl thiazoles as novel anti-Trypanosoma cruzi agents : Structural design , synthesis and pharmacological evaluation, Eur. J. Med. Chem. 86 (2014) 48–59. doi:10.1016/j.ejmech.2014.08.012.

[24] A.C.L. Leite, D.R. de M. Moreira, M.V. de O. Cardoso, M.Z. Hernandes, V.R. Alves Pereira, R.O. Silva, A.C. Kiperstok, M. da S. Lima, M.B.P. Soares, Synthesis, Cruzain docking, and in vitro studies of aryl-4-oxothiazolylhydrazones against Trypanosoma cruzi., ChemMedChem. 2 (2007) 1339–45. doi:10.1002/cmdc.200700022.

[25] D.R.M. Moreira, S.P.M. Costa, M.Z. Hernandes, M.M. Rabello, G.B. de Oliveira Filho, C.M.L. de Melo, L.F. da Rocha, C.A. de Simone, R.S. Ferreira, J.R.B. Fradico, C.S. Meira, E.T. Guimarães, R.M. Srivastava, V.R.A. Pereira, M.B.P. Soares, A.C.L. Leite, Structural investigation of anti-Trypanosoma cruzi 2-iminothiazolidin-4-ones allows the identification of agents with efficacy in infected mice., J. Med. Chem. 55 (2012) 10918–36. doi:10.1021/jm301518v.

[26] A.C.L. Leite, R.S. de Lima, D.R.D.M. Moreira, M.V.D.O. Cardoso, A.C. Gouveia de Brito, L.M. Farias Dos Santos, M.Z. Hernandes, A.C. Kiperstok, R.S. de Lima, M.B.P. Soares, Synthesis, docking, and in vitro activity of thiosemicarbazones, aminoacyl-thiosemicarbazides and acyl-thiazolidones against Trypanosoma cruzi., Bioorg. Med. Chem. 14 (2006) 3749–57. doi:10.1016/j.bmc.2006.01.034.

[27] M.E. Caputto, A. Ciccarelli, F. Frank, A.G. Moglioni, G.Y. Moltrasio, D. Vega, E.

Lombardo, L.M. Finkielsztein, Synthesis and biological evaluation of some novel 1-indanone thiazolylhydrazone derivatives as anti-Trypanosoma cruzi agents, Eur. J. Med. Chem. 55 (2012) 155–163. doi:10.1016/j.ejmech.2012.07.013.

[28] M.Z. Hernandes, M.M. Rabello, A.C.L. Leite, M.V.O. Cardoso, D.R.M. Moreira, D.J. Brondani, C.A. Simone, L.C. Reis, M.A. Souza, V.R.A. Pereira, R.S. Ferreira, J.H. McKerrow, M. Zaldini Hernandes, M. Montenegro Rabello, A. Cristina Lima Leite, M. Veríssimo Oliveira Cardoso, D. Rodrigo Magalhaes Moreira, D. José Brondani, C. Alberto Simone, L. Campos Reis, M. Assis Souza, V. Rego Alves Pereira, R. Salgado Ferreira, J. Hobson McKerrow, M.Z. Hernandes, M.M. Rabello, A.C.L. Leite, M.V.O. Cardoso, D.R.M. Moreira, D.J. Brondani, C.A. Simone, L.C. Reis, M.A. Souza, V.R.A. Pereira, Studies toward the structural optimization of novel thiazolylhydrazone-based potent antitrypanosomal agents., Bioorg. Med. Chem. 18 (2010) 7826–35. doi:10.1016/j.bmc.2010.09.056.

[29] D.R.M. Moreira, A.C. Lima Leite, M.V.O. Cardoso, R.M. Srivastava, M.Z. Hernandes, M.M. Rabello, L.F. da Cruz, R.S. Ferreira, C.A. de Simone, C.S. Meira, E.T. Guimaraes, A.C. da Silva, T.A.R. Dos Santos, V.R.A. Pereira, M.B. Pereira Soares, Structural Design, Synthesis and Structure-Activity Relationships of Thiazolidinones with Enhanced Anti-Trypanosoma cruzi Activity., ChemMedChem. 9 (2014) 177–88. doi:10.1002/cmdc.201300354.

[30] D.R. Magalhaes Moreira, A.D.T. de Oliveira, P.A.A.A. Teixeira de Moraes Gomes, C.A. de Simone, F.S. Villela, R.S. Ferreira, A.C. da Silva, T.A.R.A.R. dos Santos, M.C.A. Brelaz de Castro, V.R.A.V.R.A. Pereira, A.C.L. Leite, Conformational restriction of aryl thiosemicarbazones produces potent and selective anti-Trypanosoma cruzi compounds which induce apoptotic parasite death., Eur. J. Med.

Chem. 75 (2014) 467–78. doi:10.1016/j.ejmech.2014.02.001.

[31] D.-N. Zhang, J.-T. Li, Y.-L. Song, H.-M. Liu, H.-Y. Li, Efficient one-pot three-component synthesis of N-(4-arylthiazol-2-yl) hydrazones in water under ultrasound irradiation., Ultrason. Sonochem. 19 (2012) 475–8. doi:10.1016/j.ultsonch.2011.10.017.

[32] F. Chimenti, B. Bizzarri, E. Maccioni, D. Secci, A. Bolasco, P. Chimenti, R. Fioravanti, A. Granese, S. Carradori, F. Tosi, P. Ballario, S. Vernarecci, P. Filetici, A novel histone acetyltransferase inhibitor modulating Gcn5 network: cyclopentylidene-[4-(4'-chlorophenyl)thiazol-2-yl)hydrazone., J. Med. Chem. 52 (2009) 530–6. doi:10.1021/jm800885d.

[33] J.W.P. Espíndola, M.V. de O. Cardoso, G.B. de O. Filho, D.A. Oliveira e Silva, D.R.M. Moreira, T.M. Bastos, C.A. de Simone, M.B.P. Soares, F.S. Villela, R.S. Ferreira, M.C.A.B. de Castro, V.R.A. Pereira, S.M.F. Murta, P.A. Sales Junior, A.J. Romanha, A.C.L. Leite, Synthesis and structure–activity relationship study of a new series of antiparasitic aryloxyl thiosemicarbazones inhibiting Trypanosoma cruzi cruzain, Eur. J. Med. Chem. 101 (2015) 818–835. doi:10.1016/j.ejmech.2015.06.048.

[34] G.B. de Oliveira Filho, M.V. de O. Cardoso, J.W.P. Espíndola, D.A. Oliveira e Silva, R.S. Ferreira, P.L. Coelho, P.S. dos Anjos, E. de S. Santos, C.S. Meira, D.R.M. Moreira, M.B.P. Soares, A.C.L. Leite, Structural design, synthesis and pharmacological evaluation of thiazoles against Trypanosoma cruzi, Eur. J. Med. Chem. 141 (2017) 346–361. doi:10.1016/j.ejmech.2017.09.047.

[35] E.B. da Silva, D.A. Oliveira e Silva, A.R. Oliveira, C.H. da Silva Mendes, T.A.R. dos Santos, A.C. da Silva, M.C.A. de Castro, R.S. Ferreira, D.R.M. Moreira, M.V. de O. Cardoso, C.A. de Simone, V.R.A. Pereira, A.C.L. Leite, Desing and synthesis of

potent anti - Trypanosoma cruzi agents new thiazoles derivatives which induce apoptotic parasite death, Eur. J. Med. Chem. 130 (2017) 39–50. doi:10.1016/j.ejmech.2017.02.026.

[36] I. Franc, A. Lipinski, P.J. Feeney, C.A. Lipinski, F. Lombardo, B.W. Dominy, P.J. Feeney, Experimental and computational approaches to estimate solubility and permeability in drug discovery and development settings, Adv. Drug Deliv. Rev. 23 (1997) 3–25. doi:10.1016/S0169-409X(96)00423-1.

[37] K.M. Tyler, D.M. Engman, The life cycle of Trypanosoma cruzi revisited., Int. J. Parasitol. 31 (2001) 472–81. http://www.ncbi.nlm.nih.gov/pubmed/11334932.

[38] M.C. Fernandes, A.R. Flannery, N. Andrews, R. a Mortara, Extracellular amastigotes of Trypanosoma cruzi are potent inducers of phagocytosis in mammalian cells., Cell. Microbiol. 15 (2013) 977–91. doi:10.1111/cmi.12090.

[39] A.L. Matsuo, L.S. Silva, A.C. Torrecilhas, B.S. Pascoalino, T.C. Ramos, E.G. Rodrigues, S. Schenkman, A.C.F. Caires, L.R. Travassos, In vitro and in vivo trypanocidal effects of the cyclopalladated compound 7a, a drug candidate for treatment of Chagas' disease., Antimicrob. Agents Chemother. 54 (2010) 3318–25. doi:10.1128/AAC.00323-10.

[40] R.S. Ferreira, C. Bryant, K.K.H. Ang, J.H. McKerrow, B.K. Shoichet, A.R. Renslo, Divergent modes of enzyme inhibition in a homologous structure-activity series., J. Med. Chem. 52 (2009) 5005–8. doi:10.1021/jm9009229.

[41] X. Du, C. Guo, E. Hansell, P.S. Doyle, C.R. Caffrey, T.P. Holler, J.H. McKerrow, F.E. Cohen, Synthesis and Structure−Activity Relationship Study of Potent Trypanocidal Thio Semicarbazone Inhibitors of the Trypanosomal Cysteine Protease Cruzain, J. Med. Chem. 45 (2002) 2695–2707. doi:10.1021/jm010459j.

[42] G. Kroemer, L. Galluzzi, P. Vandenabeele, J. Abrams, E.S. Alnemri, E.H. Baehrecke, M. V Blagosklonny, W.S. El-Deiry, P. Golstein, D.R. Green, M. Hengartner, R.A. Knight, S. Kumar, S.A. Lipton, W. Malorni, G. Nuñez, M.E. Peter, J. Tschopp, J. Yuan, M. Piacentini, B. Zhivotovsky, G. Melino, Classification of cell death: recommendations of the Nomenclature Committee on Cell Death 2009., Cell Death Differ. 16 (2009) 3–11. doi:10.1038/cdd.2008.150.

[43] J.F. Tait, Imaging of apoptosis., J. Nucl. Med. 49 (2008) 1573–6. doi:10.2967/jnumed.108.052803.

[44] K.H. Jones, J.A. Senft, An improved method to determine cell viability by simultaneous staining with fluorescein diacetate-propidium iodide., J. Histochem. Cytochem. 33 (1985) 77–79. doi:10.1177/33.1.2578146.

[45] T.M. Bastos, M.I.F. Barbosa, M.M. da Silva, J.W. da C Júnior, C.S. Meira, E.T. Guimaraes, J. Ellena, D.R.M. Moreira, A.A. Batista, M.B.P. Soares, Nitro/nitrosyl-ruthenium complexes are potent and selective anti-Trypanosoma cruzi agents causing autophagy and necrotic parasite death., Antimicrob. Agents Chemother. 58 (2014) 6044–55. doi:10.1128/AAC.02765-14.

[46] V. Jimenez, R. Paredes, M.A. Sosa, N. Galanti, Natural programmed cell death in T. cruzi epimastigotes maintained in axenic cultures., J. Cell. Biochem. 105 (2008) 688–98. doi:10.1002/jcb.21864.

[47] C.A.L. Ã, Lead profiling Lead- and drug-like compounds : the rule-of-five revolution, (2004) 337–341. doi:10.1016/j.ddtec.2004.11.007.

[48] D.F. Veber, S.R. Johnson, H.-Y. Cheng, B.R. Smith, K.W. Ward, K.D. Kopple, Molecular Properties That Influence the Oral Bioavailability of Drug Candidates, J. Med. Chem. 45 (2002) 2615–2623. doi:10.1021/jm020017n.

[49] N.A. Meanwell, Improving Drug Candidates by Design: A Focus on Physicochemical Properties As a Means of Improving Compound Disposition and Safety, Chem. Res. Toxicol. 24 (2011) 1420–1456. doi:10.1021/tx200211v.

Highlights

Thirteen compounds showed good inhibition levels on the trypomastigote form of the parasite.

Six compounds present better Selective Index than benznidazole.

The cyclization of thiosemicarbazone to 1,3-thiazole improved trypanocidal activity.

Ultrastructural alterations by 1,3-thiazoles probably act via necrotic parasite cell death.